

Studies on Cu-deposited Mg Metal as a Potent Reducing Agent

March, 2012

Shinya Utsumi

The Graduate School of
Natural Science and Technology
(Doctor Course)

OKAYAMA UNIVERSITY

Contents

Chapter 1. General introduction	1
1-1. Metallic Mg	1
1-1-1. Metallic Mg as a reducing agent	1
1-1-2. Methods for activation of the metallic Mg surface	2
1-2. Mechanism of the Grignard reagent formations using metallic Mg	7
1-2-1. Consumption of the metallic Mg	7
1-2-2. Mechanism of the Grignard reagent formations	8
1-3. C-F bond activation	9
1-3-1. Reductive C-F bond activations	9
1-3-2. Metallic Mg-promoted reductive defluorination	13
1-4. General summary	17
1-5. References	20
Chapter 2. Defluorination–silylation of alkyl trifluoroacetates to 2,2-difluoro-2-(trimethylsilyl)acetates by copper-deposited magnesium and chlorotrimethylsilane	
2-1. Introduction	23
2-1-1. Difluoromethylene or trifluoromethyl moiety adjacent to carbonyl group	23
2-1-2. Methods to introduce difluoromethylene moiety adjacent to carbonyl group	24
2-1-3. Difluoroacetate (-CF ₂ CO ₂ R) moiety	25
2-1-4. A short review on difluoroacetate (-CF ₂ CO ₂ R) building blocks	26
2-2. Results and discussion	37
2-3. Summary	43
2-4. Experimental section	43
2-5. References	47
Chapter 3. Control of reductive benzylic defluorinations of (pentafluoroethyl)halobenzenes with use of Mg-Cu(0)	
3-1. Introduction	50
3-1-1. Hazard in preparations of perfluoroalkylated aryl Grignard reagents	50
3-1-2. Studies to prevent runaway reactions in Grignard reagent formation from	

perfluoroalkylated aryl halides	51
3-2. Results and discussion	53
3-2-1. Optimization of reaction conditions	53
3-2-2. Observations of Cu-deposited Mg surface	62
3-3. Conclusions	71
3-4. Experimental section	72
3-5. References	78

Chapter 4. Reductive reactions of benzotrifluoride derivatives by Cu-deposited Mg and chlorotrimethylsilane

4-1. Introduction	80
4-1-1. Conventional reductions of benzotrifluoride derivatives	80
4-2. Results and discussion	82
4-3. Conclusions	85
4-4. Experimental section	86
4-5. References	91

Appendix A. Reductive bissilylations of arylacetylenes by Cu-deposited Mg metal and chlorotrimethylsilane

92

Appendix B. Donor numbers and acceptor numbers of LiCl/DMI solvent system

97

List of publications 101

List of presentations 101

Acknowledgement 103

Chapter 1. General introduction

1-1. Metallic Mg

1-1-1. Metallic Mg as a reducing agent

Metallic Mg is a cheap, harmless, easy-to-handle, and environmental-friendly reducing agent [1]. Metallic Mg is used to form organic magnesium reagents (Grignard reagents) those are widely used to constitute C-C bonds [1b]. Additionally, Mg element is abundant in nature, thus metallic Mg is a highly available. As a reducing agent, metallic Mg has higher reduction potential ($-E^\circ = 2.4$ V) than Al ($-E^\circ = 1.7$ V) or Zn ($-E^\circ = 0.8$ V, **Figure 1-1**). The metallic Mg would be a reducing agent of high potential.

$$M^{n+} + n e^- \rightleftharpoons M(0) \quad E^\circ [V]$$

M	Li	K	Na	Mg	Al	Mn	Zn	Cr	Cd	Ni	H	Cu	Pt	Au
$-E^\circ$	3.0	2.9	2.7	2.4	1.7	1.2	0.8	0.7	0.4	0.3	0	-0.3	-1.2	-1.5

Figure 1-1. Mg and other metal reducing agents

Meanwhile, the metallic Mg has also some difficulties in their use in reductions. For example, some preparations of Grignard reagents with the metallic Mg have an induction period, or require an elevated temperature and/or vigorous stirring. Moreover, highly exothermic nature of their reactions makes them sudden and vigorous [2]. In contrast to the Li or Na metal, the metallic Mg reductions underwent rather mildly on laboratory scales, which is an advantage from the safety point of view. Because, the melting point of the metallic Mg is high enough (648 °C) to avoid melt in the course of the exothermic reductions. The difficulties of the reductions by metallic Mg are attributed to some surface conditions such as oxide layer on the metallic Mg, small amount of surface atoms of metallic

Mg than their bulk inside, lattice defects on the metallic Mg, and impurity on the metallic Mg surface [1]. The reactivity of the metallic Mg highly depends on the surface conditions of it.

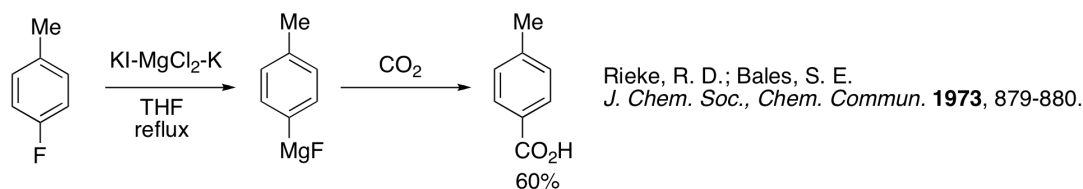
1-1-2. Methods for activation of the metallic Mg surface

Metallic Mg sometimes requires prior activation of the surface for efficient reactions, such as Grignard reagent formation [1,3]. Popular methods for the activation of metallic Mg are followings: addition of catalytic amount of iodine [4] or 1,2-dibromoethane [5], mechanical stirring [6], and ultrasonic irradiation before or during the reactions [7]. These treatments are often considered to be the methods for etch the metallic Mg surface as well as remove the oxide layer on the surface [1]. Among those popular methods, additions of iodine or 1,2-dibromoethane are very often used methods probably because they have two kinds of activating effects, removal of oxide layer on metallic Mg and self-catalytic action by resulting MgI_2 or $MgBr_2$ [9, 3a, 17].

Initial additions of MgI_2 or $MgBr_2$ also shorten induction periods of the Grignard reagent formations [9]. Garst et al. have reported prior addition of MgI_2 or $MgBr_2$ to the reacting solution showed a similar effect to that by the addition of iodine or 1,2-dibromoethane [9b]. Probably, the contribution of MgI_2 and $MgBr_2$ are similar to the “self-catalytic” action of the Grignard reagents in Grignard reagent formation [1]. A similar effect of LiCl as a “polar solute” in Grignard reagent formations was observed by Knochel et al [10]. The effects of etching surfaces of metallic Mg would contribute, because it must make “kinks and steps” on the surface, like “mechanical stirring” does. However, the net degree of the effect is unknown.

A metallic Mg with larger surface area such as powdered metallic Mg or “Rieke Mg” (metallic Mg prepared via reduction of $MgCl_2$ by potassium metal [8]) also known to promote Grignard reagent formations from “difficult” halides, such as fluorobenzenes (**Scheme 1-1**) [1, 8b]. This effect probably

comes from fast initial Grignard reagent formations for the action of a large surface area of the Mg metal.

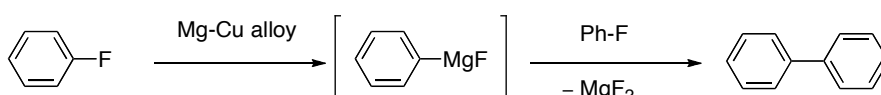


Scheme 1-1. Formation of arylmagnesium fluoride using “Rieke Mg”

Although it is not popular for these 80 years, the activation of metallic Mg by transition metals had been reported [11]. Activations of metallic Mg by forming Mg-transition metal alloys in Grignard reagent formations from *n*-butyl chloride and styryl bromide were examined by Gilman et al., in 1928 [11a]. Mg alloys with transition metals were prepared by heating metallic Mg with a transition metal and 20 wt% of iodine in an evacuated flask. Among those tested, they listed the following in the order of efficiencies: 12.75% amount of copper, 2% amount of copper, 50% amount of copper, 50% amount of tin, (ordinary Mg turnings), 10% amount of lead, 4.03% amount of manganese, and 1.83% amount of manganese. Among their tests, metallic Mg with 12.75% Cu alloy was found the best reducing agent, among examined. Formation of Mg-Cu alloy would be an important activation method because it is a different way of activation than the popular activation methods.

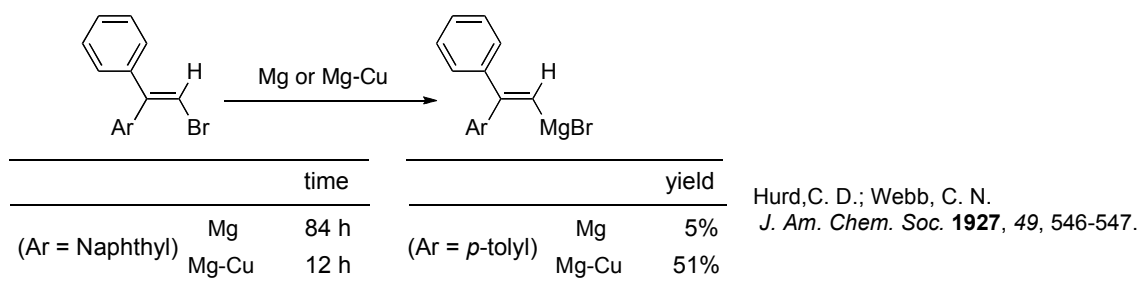
In the 1920s and the 1930s, Grignard reagent formations using the Mg-Cu alloys instead of pure Mg metal had been reported [12]. For example, the Mg-Cu method enabled Grignard reagent formation from fluorobenzene. Here, the production of the Grignard reagent was shown by the production of biphenyl (**Scheme 1-2**) [12f]. In another example, diaryl vinyl Grignard reagents were promptly formed from the corresponding bromide using Mg-Cu alloy (**Scheme 1-3**) [12a]. However,

fluoro aryl Grignard reagent formation is also possible by “Rieke Mg” (**Scheme 1-1**) [8b]. Formation of diaryl vinyl Grignard reagent formations is also possible by the use of Mg turnings activated by methyl iodide (**Scheme 1-4**) [13]. No example for the reaction that only with Mg-Cu alloy enables has been reported yet. Thus, the merit of the Mg-Cu alloys had not been recognized until now.

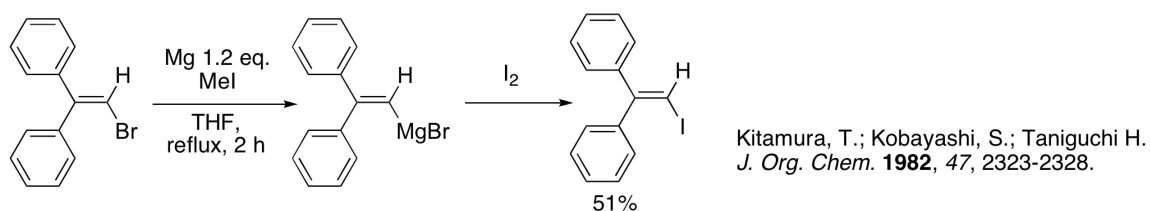


Gilman, H.; Heck, L. L. *J. Am. Chem. Soc.* **1931**, *53*, 377-378.

Scheme 1-2. A use of Mg-Cu enabled formation of phenylmagnesium fluoride.



Scheme 1-3. Diaryl vinyl Grignard reagent formations using Mg-Cu



Scheme 1-4. Diaryl vinyl Grignard reagent formation by metallic Mg with methyl iodide

Use of the Mg-Cu alloys sometimes resulted in lower yields of the Grignard reagent formation (**Table 1-1**) [12g]. Yields of Grignard reagents from various halides using the Mg-Cu alloys were investigated by Gilman et al. by acid-titration method [12g]. Yields of some Grignard reagents were

found lowered. This phenomenon had been explained by the formation of homo-coupling byproducts via Kharasch reaction [14]. This disadvantage of the lower yields of the Grignard reagents had resulted in little use of the Mg-Cu alloys.

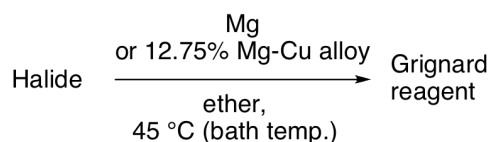
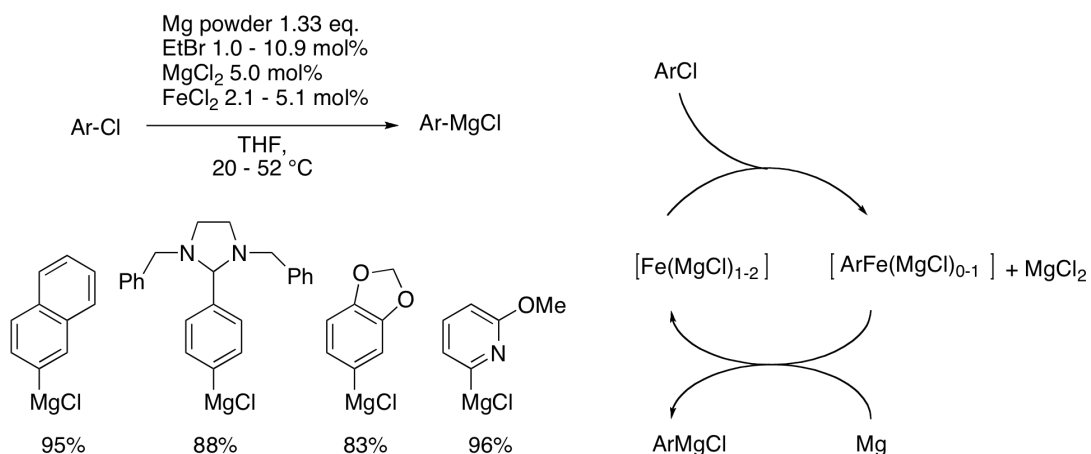


Table 1-1.

Halide	yields of Grignard reagents [%]	
	Mg-Cu	Mg
<i>n</i> -C ₄ H ₉ Br	55.4-55.8	94.0
C ₆ H ₅ CH ₂ Cl	89.5	93.1
C ₆ H ₅ Br	82.3-83.9	94.7
4-CH ₃ C ₆ H ₄ Br	92.0	86.9

Gilman, H.; Zoellner, E. A.
J. Am. Chem. Soc. **1931**, *53*, 1581-1583.

Reductive reactions with simultaneous use of metallic Mg and Cu(0) have recently been reported by Taniguchi and Onami (**Table 1-2**) [15]. The yields of the product of selenylation of aryl iodide using Cu(0) and/or metallic Mg were compared. As the result, use of stoichiometric amount of Cu or use of 10 mol% of Cu and 2 equivalent amount of metallic Mg gave the reduction product in 80% and 87% yield, respectively (entries 1 and 2). However, use of metallic Mg in the absence of Cu(0) resulted in 98% recovery of the substrate (entry 3). From these results, they proposed a plausible mechanism shown in **Scheme 1-5**. Here, the Cu metal was suggested to be oxidized by the PhSeSePh to some ionic form, and take part in the reaction as catalyst in ionic forms. The result shown in entry 3 is probably attributed to a lack of autocatalytic action of Grignard reagent caused by reactions between Grignard reagent and PhSeSePh and/or DMF. The results are also explainable by the increased reactivity of metallic Mg by Cu, like Mg-Cu alloys.



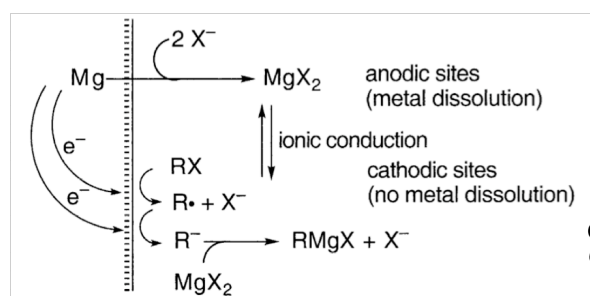
Bogdanovic, B.; Schwickardi, M.
Angew. Chem. Int. Ed. **2000**, *39*, 4610-4612.

Scheme 1-6. FeCl₂-catalyzed preparations of arylmagnesium chlorides (top left), the prepared Grignard reagents (bottom left) and their proposed mechanism (right).

1-2. Mechanism of the Grignard reagent formations using metallic Mg

1-2-1. Consumption of the metallic Mg

A widely accepted model of consumption of the metallic Mg is shown in **Figure 1-2** [18a]. Here, the reduction of organic halide (RX) and R• are driven by the dissociation of Mg(0) atom of metallic Mg into Mg²⁺ at anodic sites. In water, ionic conduction is facile, thus the anodic and cathodic sites of a consumption process could be well separated, till a macroscopic scale. In a much less polar solvent, e.g., ethers, ionic conduction should be low and the anodic and cathodic sites should be located closely. Consumption of Mg in ethereal solvents should occur near the position of the halide reduction.



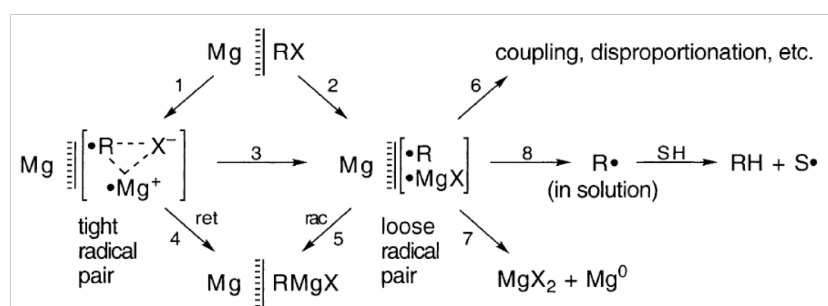
Garst, J. F.; Soriaga, M. P.
Coord. Chem. Rev. **2004**, *248*, 623-652.

Figure 1-2. A model for corrosion of metallic Mg

1-2-2. Mechanism of the Grignard reagent formations

As a result of long discussions for a few decade, the mechanism of the Grignard reagent formation had been reached to a consensus shown in **Figure 1-3**, which suggested that the Grignard reagents are formed only “on” the magnesium surface via formation of surface-bound radical species [18]. Radical species diffused from the magnesium surface ($R\cdot$ in solution) lead to formation of protonated products (via radical abstraction from solvent) or homocoupling products. The mechanism has been called the “diffusion mechanism of the Grignard reagent formation”. That is, the mechanism suggested an idea that Grignard reagents must be formed just on the magnesium surface.

Problems on the reaction pathways to the Grignard reagent ($RMgX$) formation were discussed [18, 19]. For example, rate-determining steps in alkyl Grignard reagent formations was determined to be an electron transfer step to the halides RX [20]. However, rate-determining steps in aryl Grignard reagent formations has not yet been determined. The mechanism of the aryl Grignard reagent formation is not understood completely, yet.



Garst, J. F.; Soriaga, M. P. *Coord. Chem. Rev.* **2004**, *248*, 623-652.

Figure 1-3. A consensus for mechanism of the Grignard reagent formation. Here, SH stands for a solvent.

1-3. C-F bond activation

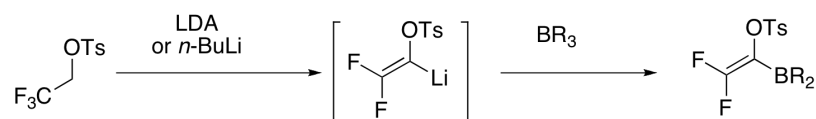
Organofluorine compounds have unique, superior properties such as chemical stability, thermo stability, surface activity, and biological activities [21]. Fluorine atom has been providing a lot of benefits to us, in the form of special products such as polymers [22] (Teflon[®]), freon, fluorinated liquid crystals [23], and pharmaceuticals. Around 10-30% of newly developed pharmaceuticals contain fluorine atom(s) in their structures in every year [24]. Nowadays, organic fluorine compounds have attracted a great deal of interest from the scientists in many fields of science and technology.

1-3-1. Reductive C-F bond activations

The C-F bonds are thermally, photochemically, electrooxidatively, and often even chemically stable (154 kcal/mol for C₆F₆) that, in general, it is not easy to cleave the C-F bonds for chemical modifications of organic fluorocompounds. The stability of the carbon-fluorine bond is exemplified by the unique property of organic perfluorocarbons such as Teflon[®]. Although a variety of C-F bond cleavage reactions have been developed [25], the bond cleavage still is considered to be tough for practical use because of their strong bonding energy.

Although the C-F bond is energetically stable, the bond can be easily cleaved when an anion center is formed at the β -position of the fluorine atom [25]. As shown in **Scheme 1-7**, abstraction of hydrogen next to the trifluoromethyl group resulted in formation of difluoroketene-type compound [26]. This reaction could be explained by the effect of negative hyperconjugation. That means, a delocalized lone-pair electrons to the low-lying σ^* -antibonding orbital of the C-F bond let get into the σ^* -orbitals of the C-F bond to cleave the bond (**Figure 1-4**, left side). The extent of the delocalization can be evaluated by the extent of overlaps between anion center orbital and $\sigma^*_{\text{C-F}}$ orbital; the bigger the overlap, the easier the C-F bond cleavage [27]. This overlap could be estimated by the *J*-coupling

between the fluorine and proton of the protonated parent compound [27].



Ichikawa, J.; Sonoda, T.; Kobayashi, H. *Tetrahedron Lett.* **1989**, *30*, 5437-5438.

Scheme 1-7. An example of defluorination

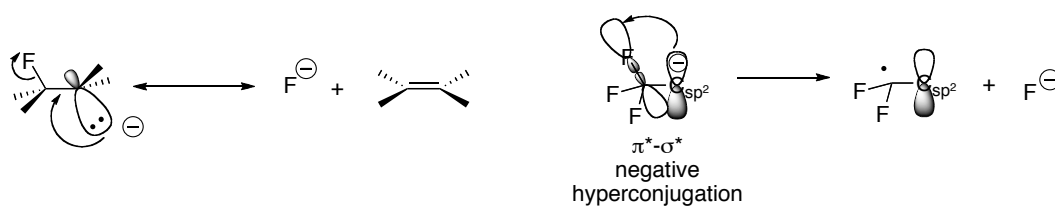
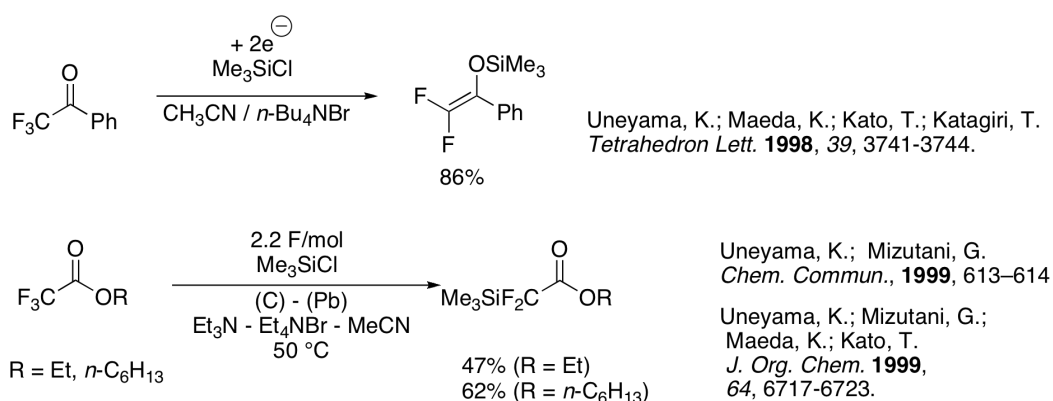


Figure 1-4. Defluorinations by forming anion at β -position of fluorine.

The C-F bond cleavages also occurred in the cases of π -anion formations at the β -positions (**Figure 1-4**, right side) [21, 29]. For example, ketones or esters having trifluoromethyl groups adjacent to their carbonyl groups can be reductively defluorinated to corresponding difluoro compounds by single electron transfer to the π -system (**Scheme 1-8**). Here, the extent of the easiness of defluorination can be explained by negative hyperconjugation between σ^* orbital of the C-F bond ($\sigma_{\text{C-F}}^*$ orbital) and the π -antibonding orbital (π^* orbital) of the conjugation system [21, 28]. The C-F bonds can be cleaved, when the electron transfer(s) into the conjugated π^* orbitals, since there are some overlaps between $\sigma_{\text{C-F}}^*$ orbitals and π^* orbitals. The only one C-F bond cleavages in the trifluoromethyl group directly attached to the π -conjugation system have been represented as “to kick out the fluorine atom by an electron” by Uneyama’s group [29c].



Scheme 1-8. Electrochemical reductive defluorinations of trifluoromethyl ketone and esters

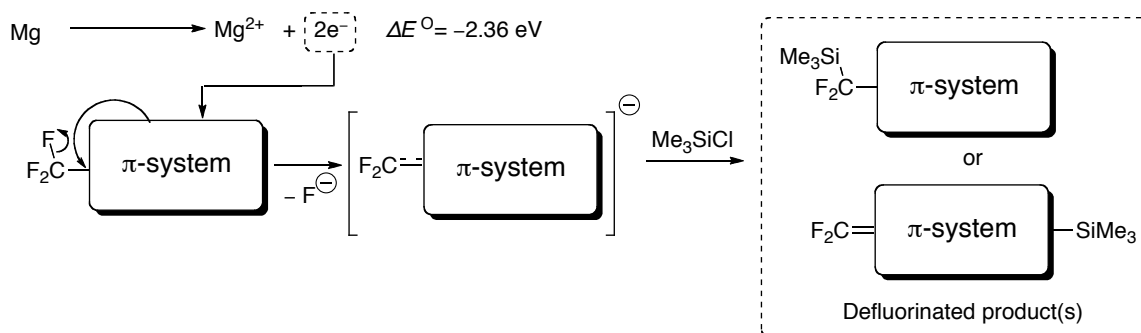
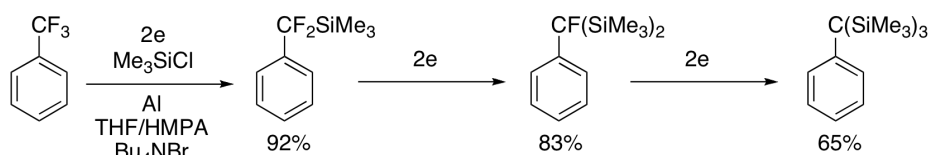


Figure 1-5. A diagram of reductive defluorination of trifluoromethylated compound

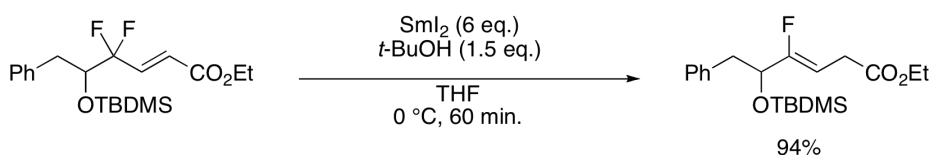
The reductive defluorination-silylation reactions can selectively remove one fluorine atom in the trifluoromethyl group with becoming a difluoro olefine as the product (**Figure 1-5**) [29, 30]. Selective defluorination-silylation reaction of aromatic trifluoromethylated compounds was reported by Clavel et al. in 1999 (electrochemical reduction of benzotrifluorides, **Scheme 1-9**) [30a]. The reaction can defluorinate and silylate the benzotrifluoride, one by one. A feature of the defluorination-silylations is selective reaction in which one fluorine atom can be removed.



Clavel, P.; Léger-Lambert, M-P.; Biran, C.; Serein-Spirau, F.; Bordeaux, M.; Roques, N.; Marzouk, H. *Synthesis*, **1999**, 829-834.

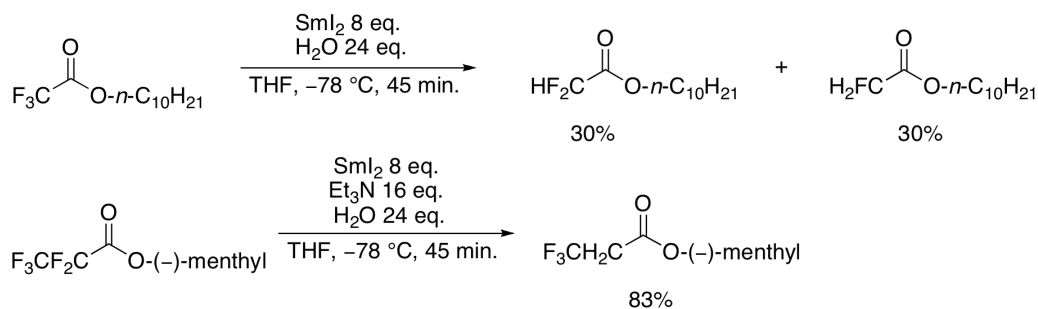
Scheme 1-9. Stepwise reductive defluorinations of benzotrifluoride

Reductive defluorination-hydration reactions by samarium(II) iodide (SmI_2) reducing agent were reported by Otaka et al. and Wettergren et al. (**Scheme 1-10** and **Scheme 1-11**), independently [31]. Reductive defluorination using the SmI_2 also removes one fluorine atom adjacent to conjugation systems such as olefins and carbonyl groups. The SmI_2 is a powerful reducing agent and can reduce even alkyl trifluoroacetates, despite of lower reducing ability of the SmI_2 ($-E^\circ = 1.55$ eV) than that of the metallic Mg ($-E^\circ = 2.4$ eV). However, lower selectivities for monofluoro- or difluoro-compounds via defluorination of trifluoroacetate by Wettergren et al. than those by electrochemical reductive silylations shown in **Scheme 1-11** [31a]. In addition, use of the SmI_2 has a problem of its cost and demands highly diluted condition (0.1 M) for avoiding unwanted decomposition of the SmI_2 agent. Although the use of the SmI_2 needs no electrochemical apparatus, the SmI_2 reagent is still tough for practical use.



Otaka, A.; Watanabe, J.; Yukimasa, A.; Sasaki, Y.; Watanabe, H.; Kinoshita, T.; Oishi, S.; Tamamura, H.; Fujii, N. *J. Org. Chem.* **2004**, *69*, 1634-1645.

Scheme 1-10. A reductive defluorination by SmI_2

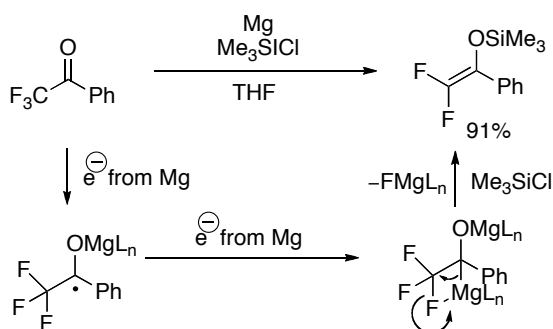


Wettergren J.; Ankner T.; Hilmersson, G. *Chem. Commun.* **2010**, 7596-7597.

Scheme 1-11. Reductive defluorinations of perfluoroalkylated esters by SmI_2

1-3-2. Metallic Mg-promoted reductive defluorination

Metallic Mg can also promote reductive C-F bond cleavages of trifluoromethyl groups attached to π -systems such as carbonyls, imines, and aromatic rings [32]. An example with a proposed mechanism is shown in **Scheme 1-12** [32a]. A feature of this method is the use of cheap metallic Mg instead of electrochemical reduction, thus, it needs no electric power supply unit, electrodes, nor a specialized reaction cell. Thus, this method is a highly available method to prepare *gem*-difluoromethylene compounds for synthetic chemists having no electrochemical apparatus.



Amii, H.; Kobayashi, T.; Hatamoto, Y.; Uneyama, K. *Chem. Commun.* **1999**, 1323-1324.

Scheme 1-12. Mg(0)-promoted reductive defluorination of α,α,α -trifluoromethylated ketones with a proposed mechanism.

Several metallic Mg-promoted reductive defluorinations of perfluoroalkylated compounds have been reported by Uneyama's group and Nishiguchi's group, independently (**Figure 1-6**) [32].

Reductive defluorinations of trifluoromethylated ketones [32a,c], aryl esters [32b], imines [32d], and aromatic compounds [32e] can afford difluoroenol silyl ethers, difluoroenamines, α -silyl acetates, and difluorobenzylsilanes, respectively. The metallic Mg-promoted reductive defluorinations would be synthetic routes to difluoromethylated compounds of wide applicabilities.

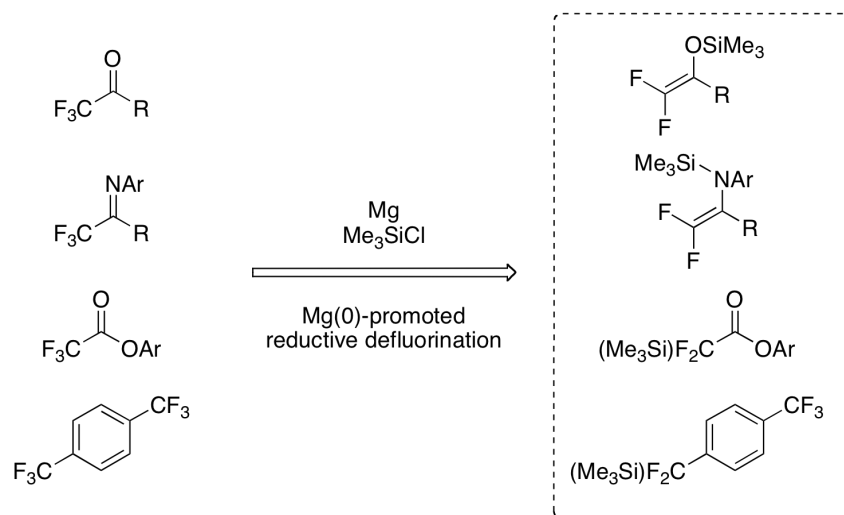


Figure 1-6. Metallic Mg-promoted reductive defluorinations and corresponding products

The reactivities of the substrates for metallic Mg-promoted reductive defluorinations had been explained by LUMO energy levels of the substrates (**Figure 1-7**) [25]. The reactivities of the substrates deduced by reaction times, conversion of the substrates, and product yields have been lined with the order of LUMO energy levels those were estimated by AM1 with MacSpartan plus package program. The **Figure 1-7** indicated that lower LUMO level of π -system of the substrate gave the defluorinated compounds in higher yields; in the case of higher LUMO level of π -system of the substrate, reductive defluorination did not occur or give products in low yields. The product yields of the metallic Mg-promoted defluorination-silylation reactions among the same type of perfluorinated compounds are consistent with the order of LUMO energy levels of the substrates. From that reason, the conversions of the reactions had been considered to be dependent on an initial electron transfer

process to a certain extent.

Meanwhile, in comparison of the reactions among the different types of the substrates, calculated LUMO energy levels were not consistent with the yields of the corresponding products. For example, (pentafluoroethyl)benzene has lower LUMO energy level (-0.48 eV) than that of α,α,α -trifluoromethyl alkyl ketone (-0.29 eV). However, the defluorination reaction of (pentafluoroethyl)benzene resulted in recovery of substrate. The reactivity of the substrates in metallic Mg-promoted defluorination reactions could not be explained only by the LUMO energy levels of the substrates. Other factors such as interactions between substrates and the surface of the metallic Mg may affect the reactivity of the substrates.

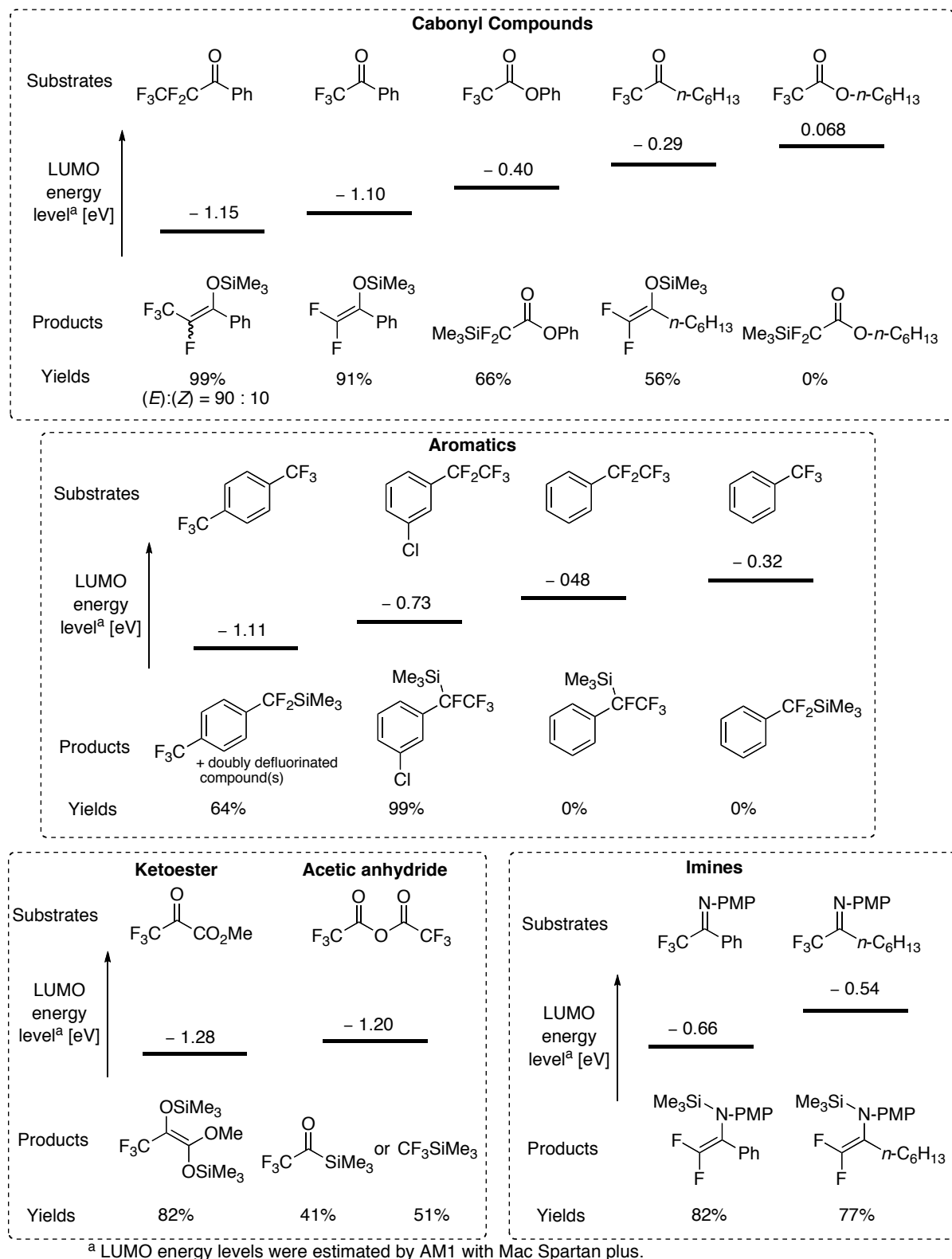
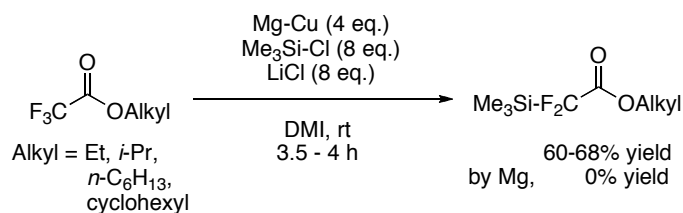


Figure 1-7. The relationships between calculated LUMO energy levels of the substrates and yields of the corresponding products

1-4. General summary

This thesis contains 3 items. In chapter 2, defluorination-silylations of alkyl trifluoroacetates to 2,2-difluoro-2-(trimethylsilyl)acetates by copper-deposited Mg metal and chlorotrimethylsilane are described (**Scheme 1-13**). In chapter 3, control of reductive defluorinations of benzylic fluorines of (pentafluoroethyl)halo benzenes with use of Cu-deposited Mg metal (**Scheme 1-14**) and microscope-observations of Cu-deposited Mg metal surfaces are described. In chapter 4, reductive defluorination-silylation reactions of substituted benzotrifluoride derivatives are described (**Scheme 1-15**).

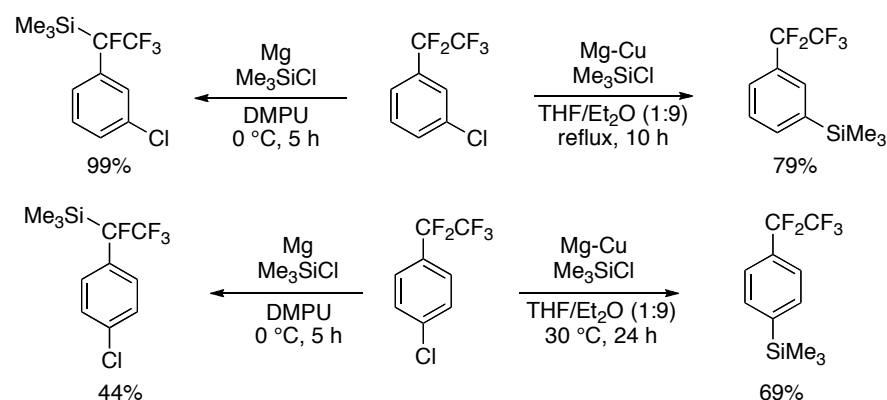
Reductive defluorination of alkyl trifluoroacetates via metallic Mg-reduction resulted in complete recovery of the substrates [32b]. The recovery of the substrates was considered to be due to limitation of the reducing ability of the metallic Mg. In the present study, reductive defluorination of alkyl trifluoroacetates were achieved by the use of Cu-deposited Mg metal instead of metallic Mg. Here, Cu-deposited Mg metal was prepared by just mixing CuCl and powdered metallic Mg in DMI solvent. The target compounds alkyl 2,2-difluoro-2-(trimethylsilyl)acetates are potential difluoromethylene building blocks. Thus, the reaction has a synthetic merit.



Scheme 1-13. Reductive defluorinations of alkyl trifluoroacetates by Cu-deposited Mg metal

In chapter 3, “control of reductive benzylic defluorinations of (pentafluoroethyl)-halo-benzenes with use of Cu-deposited Mg metal” will be described (**Scheme 1-14**). As mentioned in chapter 1-1, use of Cu-deposited Mg metal is a non-popular activation method for Grignard reagent formations.

Because of that situation, the effects of the copper deposits on Mg metal surface have not well been studied. However, in our study on “control of reductive benzylic defluorinations of (pentafluoroethyl)halobenzenes with use of Cu-deposited Mg metal”, the Cu-deposited Mg metal played an important role for selective Grignard reagent formation-type silylation with suppression of defluorination. Using Cu-deposited Mg metal enabled the selective Grignard reagent formation-type silylation of chloro-(pentafluoroethyl)benzenes even in less polar solvent, THF/Et₂O (1:9). The chemoselectivity of the reactions is consistent with “diffusion mechanism of Grignard reagents” shown in chapter 1-2-2. This plausible mechanism includes an important role of Cu(0) on the surface of metallic Mg.



Scheme 1-14. Regioselective dehalogenations of chloro(pentafluoroethyl)benzenes

In chapter 3, the surfaces of Cu-deposited Mg metal were also observed with a microscope to make the working hypothesis more certain (**Figure 1-8**). As a result, the Mg metal surfaces around Cu(0)-colored metal was consumed. These observations of surfaces of Cu-deposited Mg metal after the reactions suggested that the consumption of the Mg metal proceeded only nearby the Cu-deposits.

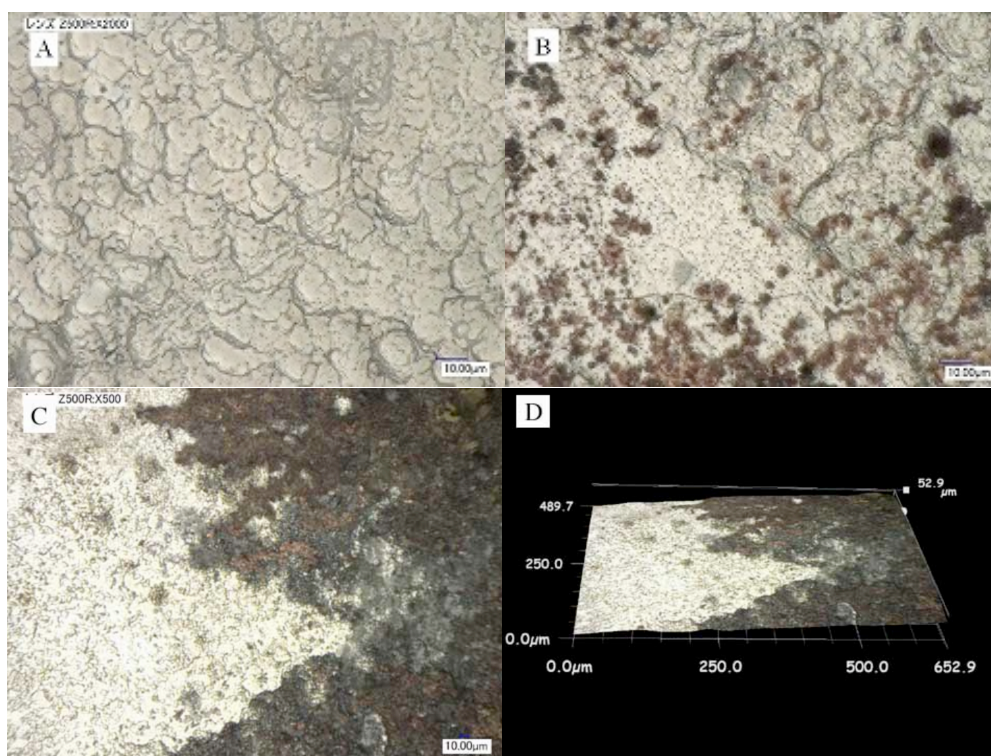
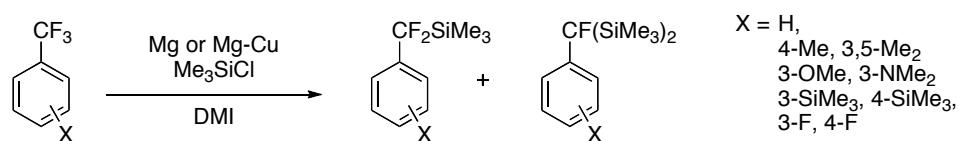


Figure 1-8. (A) $\text{Me}_3\text{Si-Cl}$ -washed metallic Mg metal surface. (B) Cu-deposited Mg metal prepared in THF and $\text{Me}_3\text{Si-Cl}$. (C) Cu-deposited Mg metal after the reaction of 3-chloro(pentafluoroethyl)benzene in THF/ Et_2O (1:9) (consumption of Mg metal was approx. 8 wt%). (D) A 3D image of **Figure 1-8C**.

Results shown in chapter 2 and 3 implied that Cu-deposited Mg metal has a higher reducing ability than the metallic Mg. However, semi-quantitative evaluation of reducing ability of Cu-deposited Mg metal has not been performed. In addition, the results shown in chapter 2 and 3 are not sufficient to reveal the mechanism of the effect of Cu(0) on Mg metal surface. From that reasons, reductive defluorinations of substituted benzotrifluorides were performed. The results of the substituent effects of the reactions are consistent with the working hypotheses shown in chapter 3.



Scheme 1-15. Reductive defluorinations of substituted benzotrifluorides by metallic Mg or Cu-deposited Mg metal

1-5. References

- [1] (a) Silverman, G. S.; Rakita, P. E. *Handbook of Grignard Reagents*, Dekker, New York, 1996. (b) Wakefield, B. J. *Organomagnesium Methods in Organic Synthesis*, Academic Press, London, 1995.
- [2] am Ende, D. J.; Clifford, P. J.; DeAntonis, D. M.; SantaMaria, C.; Brenek, S. *Org. Process Res. Dev.* **1999**, *3*, 319-329.
- [3] (a) Rieke, R. D.; Sell, M. S. in *Handbook of Grignard Reagents*, ed. Silverman, G. S.; Rakita, P. E., Dekker, New York, 1996, ch. 4, pp. 53-75. (b) Lai, Y.-H. *Synthesis* **1981**, 585-604.
- [4] Ashby, E. C.; Yu, C. *J. Organometal. Chem.* **1971**, *29*, 339-348.
- [5] Pearson, D. E.; Cowan, D.; Beckler, J. D. *J. Org. Chem.* **1959**, *24*, 504-509.
- [6] Baker, K. V.; Brown, J. M.; Hughes, N.; Skarnulis, J.; Sexton, A. *J. Org. Chem.* **1991**, *56*, 698-703.
- [7] (a) Einhorn, C.; Einhorn, J.; Luche, J. L. *Synthesis* **1989**, 787-813. (b) Luche, J. L.; Damiano, J. C. *J. Am. Chem. Soc.* **1980**, *102*, 7926-7927.
- [8] (a) Rieke, R. D.; Hudnall, P. M. *J. Am. Chem. Soc.* **1972**, *94*, 7178-7179. (b) Rieke, R. D.; Bales, S. E. *J. Chem. Soc., Chem. Commun.* **1973**, 879-880. (c) Rieke, R. D.; Bales, S. E. *J. Am. Chem. Soc.* **1974**, *96*, 1775-1781.
- [9] (a) Garst, J. F.; Lawrence, K. E.; Batlaw, R.; Boone, J. R.; Ungváry, F. *Inorg. Chim. Acta* **1994**, *222*, 365-375. (b) Gomberg, M.; Bachmann, W. E. *J. Am. Chem. Soc.* **1927**, *49*, 236-257.
- [10] (a) Krasovskiy, A.; Malakhov, V.; Gavryushin, A.; Knochel, P. *Angew. Chem. Int. Ed.* **2006**, *45*, 6040-6044. (b) Piller, F. M.; Appukkuttan, P.; Gavryushin, A.; Helm, M.; Knochel, P. *Angew. Chem. Int. Ed.* **2008**, *47*, 6802-6806. (c) Piller, F. M.; Appukkuttan, P.; Gavryushin, A.; Helm, M.; Knochel, P. *Chem. Commun.* **2010**, *46*, 4082-4084.
- [11] (a) Kharasch, M. S.; Reinmuth, O. *Grignard Reactions of Nonmetallic Substances*, Prentice-Hall, New York, 1954, pp 12. (b) Bogdanovic, B.; Schwickardi, M. *Angew. Chem. Int. Ed.* **2000**, *39*, 4610-4612. (c) Teerlinck, C. E.; Bowyer W. J. *J. Org. Chem.* **1996**, *61*, 1059-1064.
- [12] (a) Hurd, C. D.; Webb, C. N. *J. Am. Chem. Soc.* **1927**, *49*, 546-559. (b) Gilman, H.; Peterson, J. M.; Schulze, F. *Rec. Trav. Chim.* **1928**, *47*, 19-27. (c) Gilman, H.; Heck, L. L. *Bull. Soc. Chim.* **1929**, *45*, 250. (d) Kharasch, M. S.; Reinmuth, O. *Grignard Reactions of Nonmetallic Substances*, Prentice-Hall, New York, 1954, pp 11. (e) Wakefield, B. J. *Organomagnesium Method in Organic Synthesis*, Academic Press, London, 1995, pp 26. (f) Gilman, H.; Heck, L. L. *J. Am. Chem. Soc.* **1931**, *53*, 377-378. (g) Gilman, H.; Zoellner, E. A. *J. Am. Chem. Soc.* **1931**, *53*, 1581-1583. (h) Johnson, G.; Adkins, H. *J. Am. Chem. Soc.* **1931**, *53*, 1520-1523. (i) Gilman, H.; John, N. B. S. *Rec. Trav. Chim. Pays-Bas* **1930**, *49*, 717-723. (j) Case, F. H. *J. Am. Chem. Soc.* **1936**, *58*, 1246-1249. (k) Shepard, A. F.; Winslow, N. R.; Johnson, J. R. *J. Am. Chem.*

- Soc.* **1930**, 52, 2083-2090. (l) Takeda, A.; Shinhama, K.; Tsuboi, S. *Bull. Chem. Soc. Jpn.* **1977**, 50, 1903-1904.
- [13] Kitamura, T.; Kobayashi, S.; Taniguchi, H. *J. Org. Chem.* **1982**, 47, 2323-2328.
- [14] Kharasch, M. S.; Kleiger, S. C.; Martin, J. A.; May, F. R. *J. Am. Chem. Soc.* **1941**, 63, 2305-2307.
- [15] Taniguchi, N.; Onami, T. *J. Org. Chem.* **2004**, 69, 915-920.
- [16] (a) Aleandri, L. E.; Bogdanovic, B.; Bons, P.; Dürr, C.; Gaidies, A.; Hartwig, T.; Huckett, S. C.; Lagarden, M.; Wilczok, U. *Chem. Mater.* **1995**, 7, 1153-1170. (b) Aleandri, L. E.; Bogdanovic, B.; Dürr, C.; Jones, D. J.; Roziere, J.; Wilczok, U. *Adv. Mater.* **1996**, 8, 600-604. (c) Aleandri, L. E.; Bogdanovic, B.; Dürr, C.; Huckett, S. C.; Jones, D. J.; Kolb, U.; Lagarden, M.; Roziere, J.; Wilczok, U. *Chem. Eur. J.* **1997**, 3, 1710-1718. (d) Bogdanovic, B.; Leitner, W.; Six, C.; Wilczok, U.; Wittmann, K. *Angew. Chem. Int. Ed. Engl.* **1997**, 36, 502-504.
- [17] Teerlinck, C. E.; Bowyer W. J. *J. Org. Chem.* **1996**, 61, 1059-1064.
- [18] (a) Garst, J. F.; Soriaga, M. P. *Coord. Chem. Rev.* **2004**, 248, 623-652. (b) Walborsky, I. M.; Aronoff, M. S. *J. Organomet. Chem.* **1973**, 51, 31-53.
- [19] Andrieux, C. P.; Gorande, A. L.; Savéant, J-M. *J. Am. Chem. Soc.* **1992**, 114, 6892-6904.
- [20] Rogers, R. J.; Mitchell, H. L.; Fujiwara, Y.; Whitesides, G. M. *J. Org. Chem.* **1974**, 39, 857-859.
- [21] Uneyama, K. *Organofluorine Chemistry* Blackwell publishing: Oxford, 2006.
- [22] (a) Ameduri, B. *Chem. Rev.* **2009**, 109, 6632-6686. (b) Kharitonov, A.P. *J. Fluorine Chem.* **2000**, 103, 123-127.
- [23] (a) Krafft, M. P.; Riess J. G. *Chem. Rev.* **2009**, 109, 1714-1792. (b) Dolbier W. R. Jr. *J. Fluorine Chem.* **2005**, 126, 157-163.
- [24] (a) Hagmann, W. K. *J. Med. Chem.* **2008**, 51, 4359-4369. (b) Purser, S.; Moore, P. R.; Swallow, S.; Gouverneur, V. *Chem. Soc. Rev.* **2008**, 37, 320-330. (c) Begue, J-P.; Bonnet-Delpon, D. *J. Fluorine Chem.* **2006**, 127, 992-1012.
- [25] Amii, H.; Uneyama, K. *Chem. Rev.* **2009**, 109, 2119-2183, and references therein.
- [26] Ichikawa, J.; Sonoda, T.; Kobayashi, H. *Tetrahedron Lett.* **1989**, 30, 5437-5438.
- [27] Uneyama, K.; Katagiri, T.; Amii, H. *Acc. Chem. Res.* **2008**, 41, 817-829.
- [28] (a) Roberts, J. D.; Webb, R. L.; McElhill, E. A. *J. Am. Chem. Soc.* **1950**, 72, 408-411. (b) Adcock, W.; Andrieux, C. P.; Clark, C. I.; Neudeck A.; Savéant, J-M.; Tardy, C. *J. Am. Chem. Soc.* **1995**, 117, 8285-8286. (c) Antonello, S.; Maran, F. *Chem. Soc. Rev.* **2005**, 34, 418-428.
- [29] (a) Uneyama, K.; Maeda, K.; Kato, T.; Katagiri, T. *Tetrahedron Lett.* **1998**, 39, 3741-3744. (b) Uneyama, K.; Mizutani, G. *Chem. Commun.* **1999**, 613-614. (c) Uneyama, K.; Mizutani, G.; Maeda, K.; Kato, T. *J. Org. Chem.* **1999**, 64, 6717-6723.

- [30] (a) Clavel, P.; Léger-Lambert, M-P.; Biran, C.; Serein-Spirau, F.; Bordeau, M.; Roques, N.; Marzouk, H. *Synthesis* **1999**, 829-834. (b) Clavel, P.; Lessene, G.; Biran, C.; Bordeau, M.; Roques, N. Trévin, S.; de Montauzon, D. *J. Fluorine Chem.* **2001**, *107*, 301-310.
- [31] (a) Wettergren J.; Ankner T.; Hilmersson, G. *Chem. Commun.* **2010**, 7596-7597. (b) Otaka, A.; Watanabe, J.; Yukimasa, A.; Sasaki, Y.; Watanabe, H.; Kinoshita, T.; Oishi, S.; Tamamura, H.; Fujii, N. *J. Org. Chem.* **2004**, *69*, 1634-1645.
- [32] (a) Amii, H.; Kobayashi, T.; Hatamoto, Y.; Uneyama, K. *Chem. Commun.* **1999**, 1323-1324. (b) Amii, H.; Kobayashi, T.; Uneyama, K. *Synthesis* **2000**, 2001-2003. (c) Amii, H.; Kobayashi, T.; Terasawa, H.; Uneyama, K. *Org. Lett.* **2001**, *3*, 3103-3105. (d) Kobayashi, K.; Nakagawa, T.; Amii, H.; Uneyama, K. *Org. Lett.* **2003**, *5*, 4297-4300. (e) Amii, H.; Hatamoto, Y.; Seo, M.; Uneyama, K. *J. Org. Chem.* **2001**, *66*, 7216-7218. (f) Nakamura, Y.; Uneyama, K. *J. Org. Chem.* **2007**, *72*, 5894-5897. For a review, see (g) Uneyama, K.; Amii, H. *J. Fluorine Chem.* **2002**, *114*, 127-131.

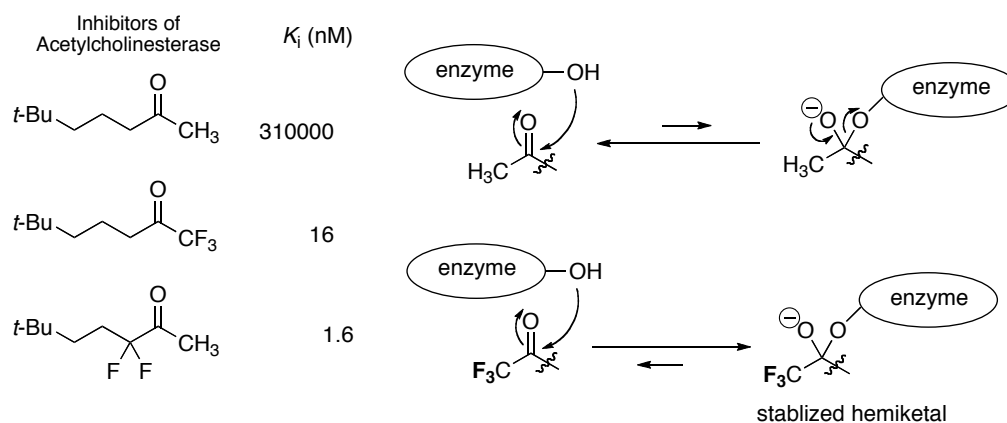
Chapter 2. Defluorination–silylation of alkyl trifluoroacetates to 2,2-difluoro-2-(trimethylsilyl)acetates by Cu-deposited Mg metal and chlorotrimethylsilane

2-1. Introduction

2-1-1. Difluoromethylene or trifluoromethyl moiety adjacent to carbonyl group

The presence of three or two fluorinated-methyl moiety adjacent to carbonyl functionality increases the electrophilicity of the carbonyl carbon atom and facilitates the addition of nucleophiles (**Scheme 2-1**) [1]. Nucleophilic addition of an enzyme active site to the carbonyl group of fluorinated ketones has been suggested to be responsible for the inhibition of a variety of enzymes [2]. The promotion for trapping the hydroxyl group of some enzymes by the trifluoroacetyl group (strong electron withdrawing group) and abnormal stabilization of the hemiacetal form by the group lead to remarkable inhibition activities compared to the corresponding acyl compounds [2d]. This inhibition can be also observed in cases of corresponding difluoro compound, and in some cases, the inhibitory effect becomes stronger than that of trifluoromethyl acetyl compounds [2d]. Difluoromethylene or trifluoromethyl groups adjacent to carbonyl functionality can dramatically change the inhibitory activities of some enzymes by their strong electronegativity.

Some examples of pharmaceutical drugs involving difluoromethylene neighboring carbonyl groups in the structures are shown (**Figure 2-1**). Difluoro peptidyl motif has been used as the key component for potent and selective renin inhibitors [3], and HIV-1 protease inhibitors [4]. As other examples, difluoro β -lactam unit is used in human leukocyte elastase inhibitors [5], and β -lactamase inhibitors [6]. The difluoromethylene unit could be a key structure of inhibitory pharmaceuticals.



Gelb, M. H.; Svaren, J. P.; Abeles, R. H. *Biochemistry* **1985**, *24*, 1813-1817.

Scheme 2-1. An effect of fluorine atoms in enzyme inhibitors

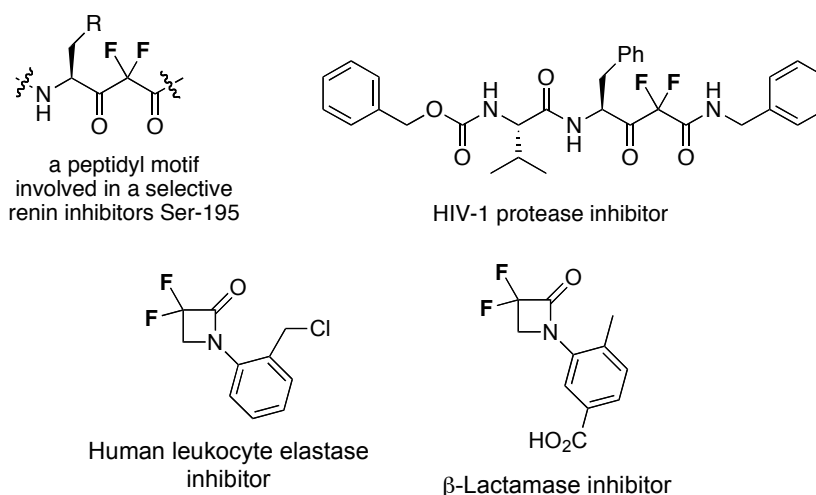


Figure 2-1. Examples of pharmaceutical drugs involving α,α -difluorocarbonyl moiety

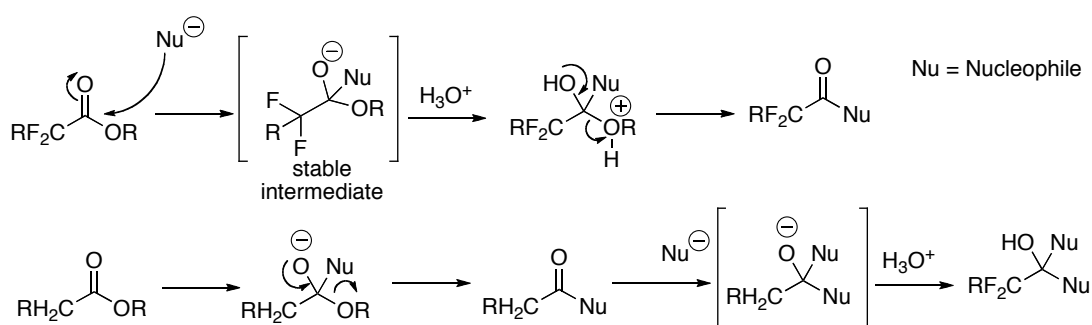
2-1-2. Methods to introduce difluoromethylene moiety adjacent to carbonyl group

Popular methods to introduce a difluoromethylene moiety adjacent to a carbonyl group are categorized into 4 types, as follows. (1) defluorination of trifluoromethyl moiety adjacent to carbonyl moiety to difluoromethylene moiety [7], (2) use of difluoromethylene building blocks such as bromodifluoroacetates [8], (3) constructions of carbonyl group adjacent to difluoromethylene moiety [9], (4) fluorination of ketoester, enols or enamines using fluorinating agents [10], such as F_2 [10d], XeF_2 [10e], ClO_4F [10f], $(CF_3SO_2)_2NF$ [10g], NF_3O [10h], BrF_3 [10i], DAST [10j], and SelectfluorTM

[10k-m]. In section 2-1-4, (1) conventional defluorination of trifluoromethyl moiety to difluoromethylene moiety and (2) conventional use of the difluoromethylene building blocks such as bromodifluoroacetates will be discussed.

2-1-3. Difluoroacetate (-CF₂CO₂R) moiety

Difluoroacetate (CF₂CO₂R) can be converted to various difluoroketone or difluoroamide via nucleophilic additions (**Scheme 2-2**) [11]. Nucleophilic additions to carbonyl carbon of CF₂CO₂R groups normally give corresponding carbonyl compounds instead of doubly attacked alcohols. This selective addition is attributed to stable anion intermediates formed after the first nucleophilic additions to the carbonyl carbons, which is induced by strong electron withdrawing effect of the difluoromethylene group. Thus, difluoroacetate (CF₂CO₂R) can be used as versatile precursors for various α,α-difluorocarbonyl moieties such as α,α-difluoroketones (-CF₂C(=O)-C) and α,α-difluoroamides (-CF₂C(=O)-N). Thus, the introduction of difluoroacetate is an important subject for preparations of α,α-difluorocarbonyl compounds.



Scheme 2-2. Substituent effect of fluorine atoms adjacent to carbonyls in nucleophilic additions

2-1-4. A short review on difluoroacetate (-CF₂CO₂R) building blocks

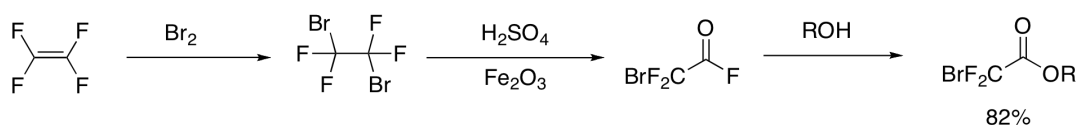
To date, several difluoroacetate building blocks have been developed. Some of them are commercially available (e.g. 2-bromo-2,2-difluoroacetates (BrCF₂CO₂R) and 2-chloro-2,2-difluoroacetates (ClCF₂CO₂R)). In this section, four representative difluoroacetate building blocks, BrCF₂CO₂R, ClCF₂CO₂R, difluoroketene silylactal, and 2,2-difluoro-2-(trimethylsilyl)acetates (Me₃Si-CF₂CO₂R) are reviewed including their selected usages. Their advantage and disadvantages are also described.

2-1-4-1. 2-Bromo-2,2-difluoroacetates (BrCF₂CO₂R)

2-Bromo-2,2-difluoroacetates (BrCF₂CO₂R) are popular, versatile building blocks for -CF₂(C=O)- unit. Ethyl 2-bromo-2,2-difluoroacetate (BrCF₂CO₂Et) is commercially available, and it has been utilized in more than 1,000 reactions up to now (More than 1,000 C-C bond forming reactions of BrCF₂CO₂Et could be found by SciFinder[®]).

A preparative method (manufacturing method) for 2-bromo-2,2-difluoroacetates (BrCF₂CO₂R)

The BrCF₂CO₂R has been manufactured from tetrafluoroethylene via bromination and subsequent Fe₂O₃-catalyzed decomposition by fuming sulfuric acid and esterification (**Scheme 2-3**) [12]. The BrCF₂CO₂Et is commercially available, however, more expensive (¥113,700/mol, TCI) than 2-chloro-2,2-difluoroacetate (ClCF₂CO₂R, ¥45,700/mol TCI).

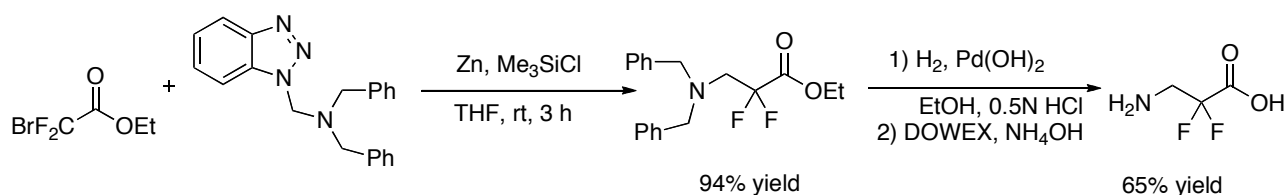


Scheme 2-3. A manufacturing processes for 2-bromo-2,2-difluoroacetates

Representative Reactions using 2-bromo-2,2-difluoroacetates ($\text{BrCF}_2\text{CO}_2\text{R}$)

The 2-bromo-2,2-difluoroacetate ($\text{BrCF}_2\text{CO}_2\text{R}$) is a versatile $-\text{CF}_2(\text{C}=\text{O})-$ building blocks. 2-Bromo-2,2-difluoroacetates ($\text{BrCF}_2\text{CO}_2\text{R}$) are used for introduction of $-\text{CF}_2\text{CO}_2\text{R}$ groups via Reformatsky reactions [13], Ullmann-coupling additions [14], radical additions initiated by an electron transfer [15] and metal-catalyzed cross coupling reactions [16] (Scheme 2-4, 2-5, 2-6, and 2-7, respectively). The $\text{BrCF}_2\text{CO}_2\text{R}$ can be used for preparations of β -lactams and subsequent synthesis of difluorinated amino acids (Scheme 2-8 and Scheme 2-9) [17]. Thus, $\text{BrCF}_2\text{CO}_2\text{R}$ is a versatile agent to introduce $-\text{CF}_2\text{CO}_2\text{R}$ groups, probably the most frequently used $-\text{CF}_2\text{CO}_2\text{R}$ building block.

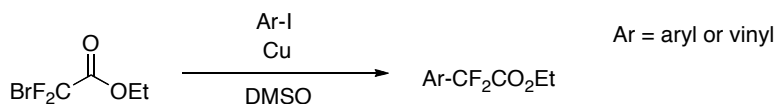
Reformatsky reaction



Hallinan, E. A.; Fried, J. *Tetrahedron Lett.* **1984**, *25*, 2301-2302.
Cheguillaume, A.; Lacroix, S.; Jacqueline Marchand-Brynaert, J. *Tetrahedron Lett.* **2003**, *44*, 2375-2377.

Scheme 2-4. A Reformatsky reaction using $\text{BrCF}_2\text{CO}_2\text{R}$

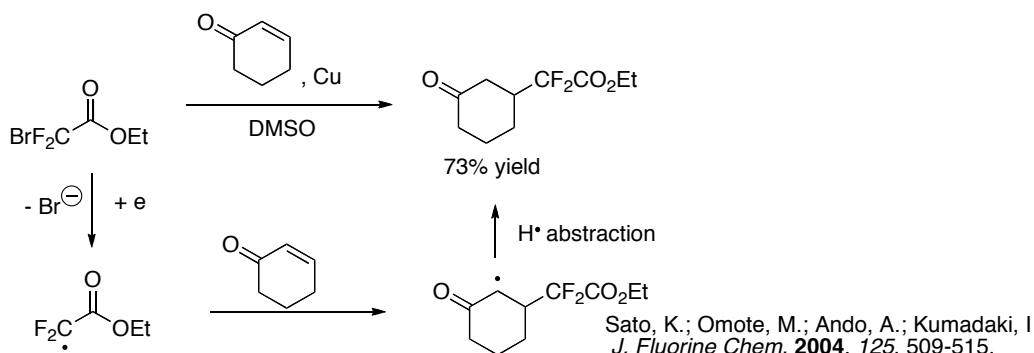
Ullmann coupling reaction



Sato, K.; Omote, M.; Ando, A.; Kumadaki, I. *J. Fluorine Chem.* **2004**, *125*, 509-515.

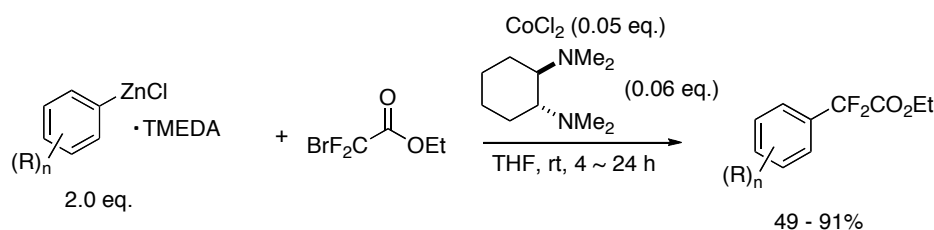
Scheme 2-5. An Ullmann coupling reaction using $\text{BrCF}_2\text{CO}_2\text{R}$

Radical addition

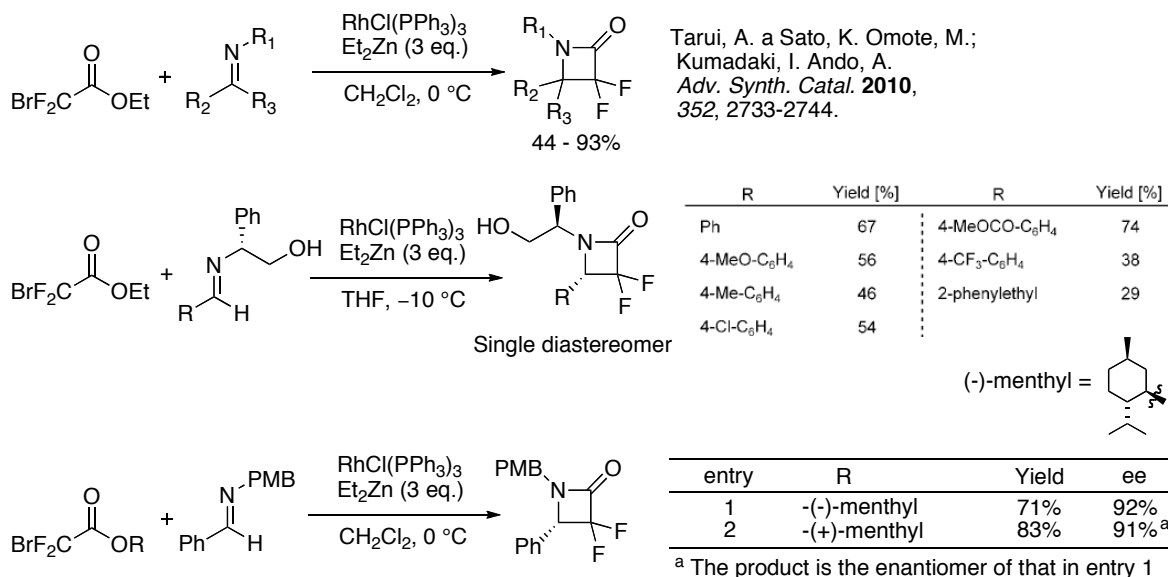


Scheme 2-6. A radicalic C-C bond formation of $\text{BrCF}_2\text{CO}_2\text{R}$

Metal-catalyzed cross coupling reactions

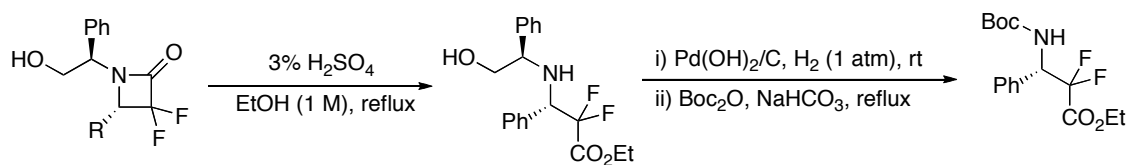


Scheme 2-7. A metal-catalyzed cross coupling reaction using $\text{BrCF}_2\text{CO}_2\text{R}$



A. Tarui, D. Ozaki, N. Nakajima, Y. Yokota, Y. S. Sokeirek, K. Sato, M. Omote, I. Kumadaki, A. Ando, *Tetrahedron Lett.* **2008**, 49, 3839–3843.

Scheme 2-8. Syntheses of difluoro β -lactams from $\text{BrCF}_2\text{CO}_2\text{R}$



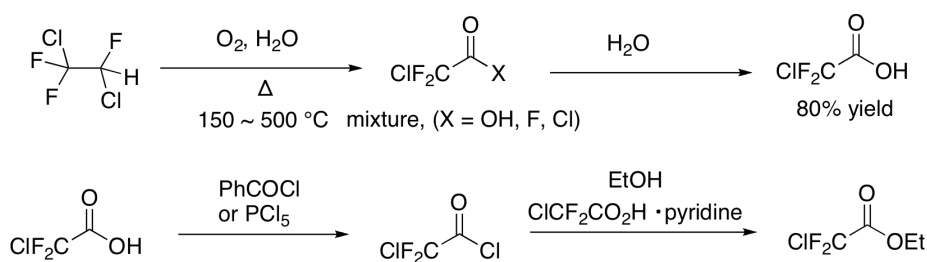
Tarui, A. a Sato, K. Omote, M.; Kumadaki, I. Ando, A. *Adv. Synth. Catal.* **2010**, *352*, 2733-2744.

Scheme 2-9. A ring-opening reaction of a difluoro β -lactam and synthesis of amino acid derivative

2-1-4-2. 2-Chloro-2,2-difluoroacetates ($\text{ClCF}_2\text{CO}_2\text{R}$)

Preparative method (manufacturing method) for 2-chloro-2,2-difluoroacetates ($\text{ClCF}_2\text{CO}_2\text{R}$)

The 2-chloro-2,2-difluoroacetate ($\text{ClCF}_2\text{CO}_2\text{R}$) can also be used as a difluoroacetate building block. The 2-chloro-2,2-difluoroacetate ($\text{ClCF}_2\text{CO}_2\text{R}$) is manufactured from commercially available 1,2-dichloro-1,1,2-difluoroethane (**Scheme 2-10**) via 2 steps [18]. Commercially available ethyl 2-chloro-2,2-difluoroacetate ($\text{ClCF}_2\text{CO}_2\text{Et}$) is cheaper than $\text{BrCF}_2\text{CO}_2\text{R}$. However, the reactions using $\text{ClCF}_2\text{CO}_2\text{Et}$ requires harsher conditions than that for $\text{BrCF}_2\text{CO}_2\text{Et}$. Probably from this reason as well as a weaker reactivity, the $\text{ClCF}_2\text{CO}_2\text{Et}$ has not been frequently used than $\text{BrCF}_2\text{CO}_2\text{Et}$.

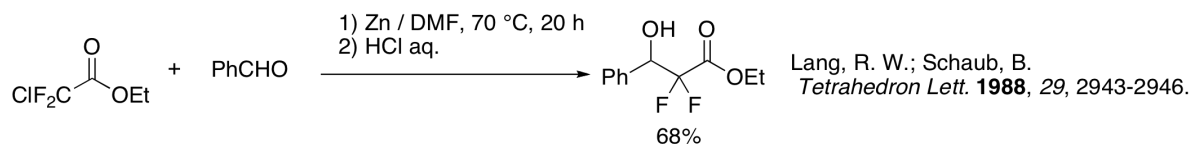


Scheme 2-10. A manufacturing method for 2-chloro-2,2-difluoroacetates

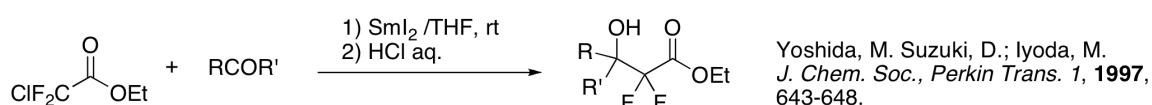
Representative Reactions using 2-chloro-2,2-difluoroacetates

The 2-chloro-2,2-difluoroacetates ($\text{ClCF}_2\text{CO}_2\text{R}$) can be used as difluoromethylene building block via radicalic addition initiated by an electron transfer reduction. Here, the reducing agents of the

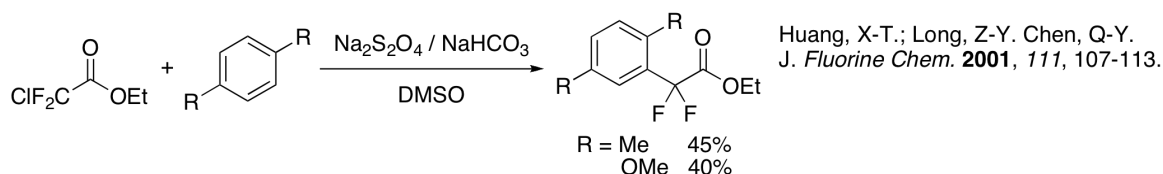
electron transfer reduction were Zn metal (via Barbier-type reaction under high temperature conditions) [19], SmI₂ [20], and Na₂S₂O₄ [21] (**Scheme 2-11**, **2-12**, and **Scheme 2-13**, respectively).



Scheme 2-11. An example of Reformatsky-type addition of 2-chloro-2,2-difluoroacetates using Zn



Scheme 2-12. An example of Reformatsky-type addition of 2-chloro-2,2-difluoroacetates using SmI₂

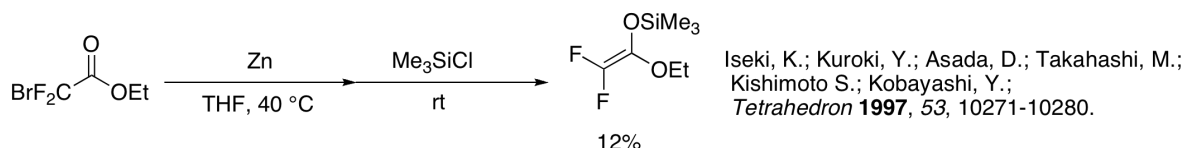


Scheme 2-13. Examples of radicalic C-C bond formations of 2-chloro-2,2-difluoroacetates

2-1-4-3. Difluoroketene silylacetal (CF₂=C(OSiMe₃)(OR))

A preparative method of difluoroketene silylacetal

The difluoroketene silylacetal was prepared by reduction of ethyl 2-bromo-2,2-difluoroacetate by activated zinc powder and subsequent treatment by chlorotrimethylsilane (**Scheme 2-14**) [22]. However, the difluoroketene silylacetal is so moisture-sensitive that the yield via the method remains low (12%).

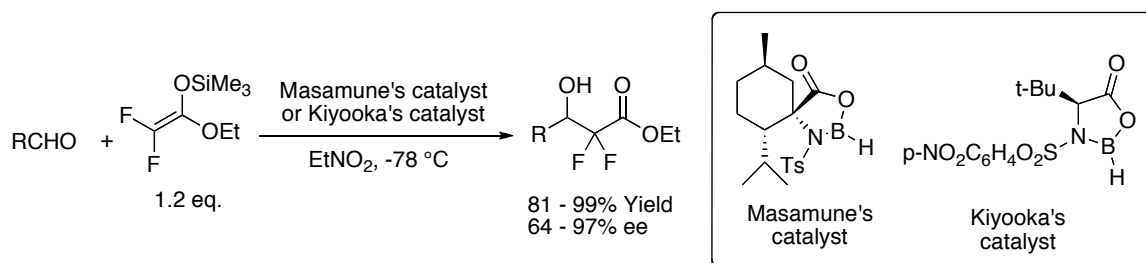


Scheme 2-14. A reductive preparation of difluoroketene silylacetal

Representative reactions of difluoroketene silylacetals

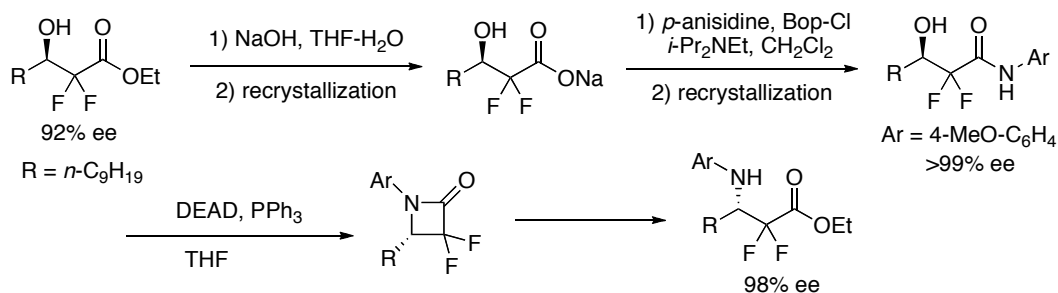
The difluoroketene silylacetal could be utilized for asymmetric Mukaiyama aldol reactions (Scheme 2-15) [22, 23]. Asymmetric aldol reactions with aldehydes gave the aimed adduct in 81-99% yield and 64~97% ee under low temperature conditions. The chiral adduct was used as a precursor of difluoro β -amino acids (Scheme 2-16). Thus, difluoroketene silylacetal is also a synthetically important $-\text{CF}_2\text{CO}_2\text{R}$ building block.

Mukaiyama aldol reaction



Iseki, K.; Kuroki, Y.; Asada, D.; Kobayashi, Y. *Tetrahedron Lett.* **1997**, *38*, 1447.
Iseki, K.; Kuroki, Y.; Asada, D.; Takahashi, M.; Kishimoto, S.; Kobayashi, Y. *Tetrahedron* **1997**, *53*, 10271-10280.
Iseki, K. *Tetrahedron* **1998**, *54*, 13887.

Scheme 2-15. Mukaiyama aldol reaction of difluoroketene silylacetal

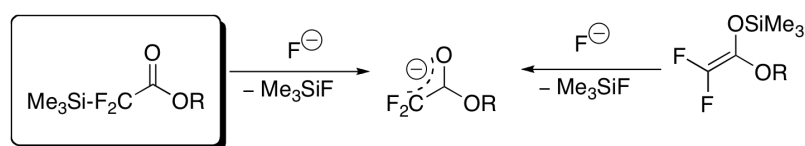


Iseki, K.; Kuroki, Y.; Asada, D.; Takahashi, M.; Kishimoto, S.; Kobayashi, Y. *Tetrahedron* **1997**, *53*, 10271-10280.

Scheme 2-16. Syntheses of difluoro- β -lactams from the aldol-adduct.

2-1-4-4. 2,2-difluoro-2-(trimethylsilyl)acetates ($\text{Me}_3\text{Si-CF}_2\text{CO}_2\text{R}$)

2,2-Difluoro-2-(trimethylsilyl)acetate is a potential difluoromethylene building block [24,25]. 2,2-Difluoro-2-(trimethylsilyl)acetate was proposed as an alternative of difluoroketene silyl acetal (**Scheme 2-17**) [24f]. Furthermore, 2,2-difluoro-2-(trimethylsilyl)acetate is storable at room temperature and not moisture-sensitive unlike difluoroketene silyl acetal. However, the 2,2-difluoro-2-(trimethylsilyl)acetate has not well been used as difluoromethylene building blocks, because of the lack of their large-scale preparative method.

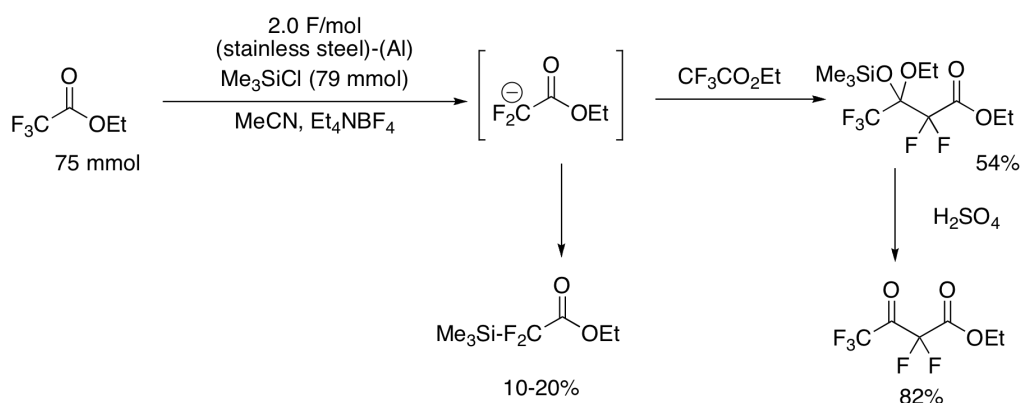


Scheme 2-17. 2,2-Difluoro-2-(trimethylsilyl)acetates as difluoromethylene building block

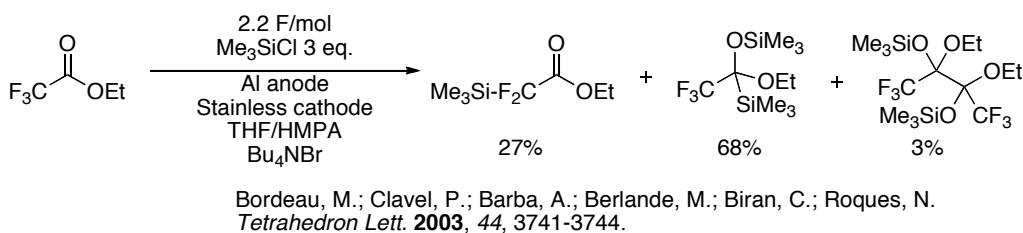
Preparative methods for 2,2-difluoro-2-(trimethylsilyl)acetates ($\text{Me}_3\text{Si-CF}_2\text{CO}_2\text{R}$)

Ethyl 2,2-difluoro-2-(trimethylsilyl)acetates were prepared via electrochemical synthesis from trifluoroacetates or 2-chloro-2,2-difluoroacetates by three groups, Stepanov's group, Bordeaux's group and Uneyama's group [24]. Stepanov et al. reported that ethyl 2,2-difluoro-2-(trimethylsilyl)acetate was obtained in 10-20% as a byproduct of Claisen-type compound (**Scheme 2-18**) [24a]. The Bordeaux's procedure prepared difluoroacetate as a minor product in up to 27% yield (**Scheme 2-19**) [24c]. Meanwhile, the electrochemical reduction of 2-chloro-2,2-difluoroacetates gives the aimed difluoro compound in 70% isolated yield (**Scheme 2-20**) [24b]. Uneyama's procedure, electrochemical reduction of ethyl trifluoroacetate, gave ethyl 2,2-difluoro-2-trimethylsilylacetate in 47% isolated yield (**Scheme 2-21**) [24e]. An advantage of the Uneyama's method is use of

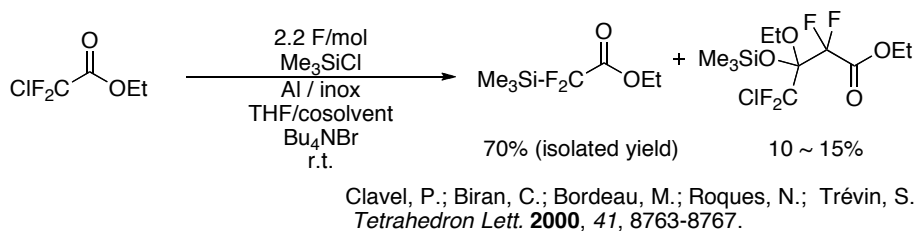
commercially available and cheap alkyl trifluoroacetates (A price of $\text{CF}_3\text{CO}_2\text{Et}$ is ¥19,900/mol, TCI). Meanwhile, reduction by $\text{Mg}(0)$ of *n*-hexyl trifluoroacetate was reported to be recovery of the substrate (**Table 2-1**) [24f]. Successful reduction of trifluoroacetates by $\text{Mg}(0)$ demands alteration of alkyloxycarbonyl group to aryloxycarbonyl group. However, aryl trifluoroacetates are easy to decompose (via hydrolysis). Thus, preparation of ethyl 2,2-difluoro-2-(trimethylsilyl)acetate from ethyl trifluoroacetate via Mg -reduction has been highly demanded.



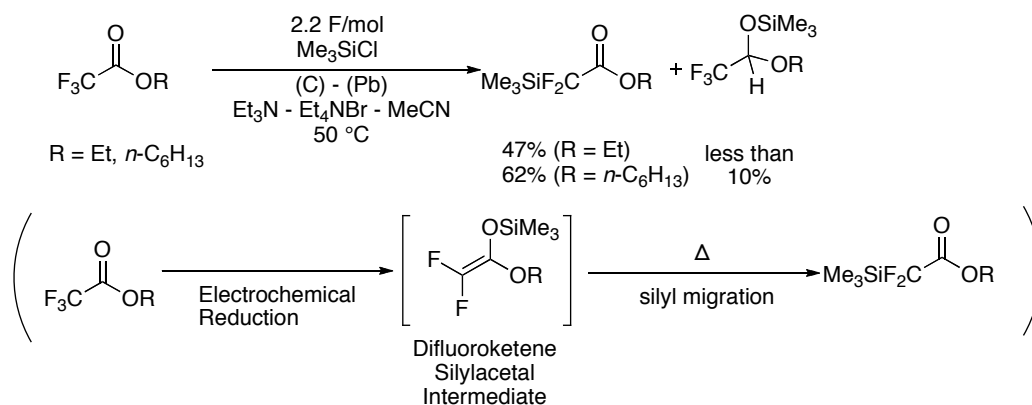
Scheme 2-18. An electroreduction of ethyl trifluoroacetate to Claisen-type compound



Scheme 2-19. An electroreduction of ethyl trifluoroacetate to a silyl ketal



Scheme 2-20. Electrochemical synthesis of 2,2-difluoro-2-(trimethylsilyl)acetates from ethyl 2-chloro-2,2-difluoroacetate



Scheme 2-21. Electrochemical synthesis of 2,2-difluoro-2-(trimethylsilyl)acetates from ethyl trifluoroacetate

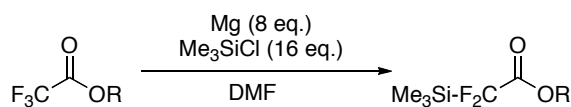


Table 2-1.

entry	R	Conditions	Isolated yields
1	C ₆ H ₁₃	rt, 24 h	0%
2	Ph	rt, 2.5 h	66%
3	Ph	rt, 2.5 h	63%
4	4-MeOC ₆ H ₄	rt, 6.5 h	64%
5	4-MeC ₆ H ₄	rt, 4.5 h	56%
6	4-ClC ₆ H ₄	rt, 1.5 h	55%

Amii, H. Kobayashi, T.; Uneyama, K. *Synthesis* **2000**, 2001-2003.

Representative reactions using 2,2-difluoro-2-(trimethylsilyl)acetates

The 2,2-difluoro-2-(trimethylsilyl)acetates were used as difluoromethylene building blocks (**Figure 2-2**) [24b, 24e, 25]. Fluoride-catalyzed nucleophilic additions to aldehydes, ketones, acyl chlorides and an imine were reported by several groups [25]. Nucleophilic additions to benzyl bromide and vinyl chloride by KF/CuI system have also been reported [24e]. Alkyl 2,2-difluoro-2-(trimethylsilyl)acetates was used similarly to the Ruppert-Prakash reagent (CF₃-SiMe₃), a popular trifluoromethylating agent [26].

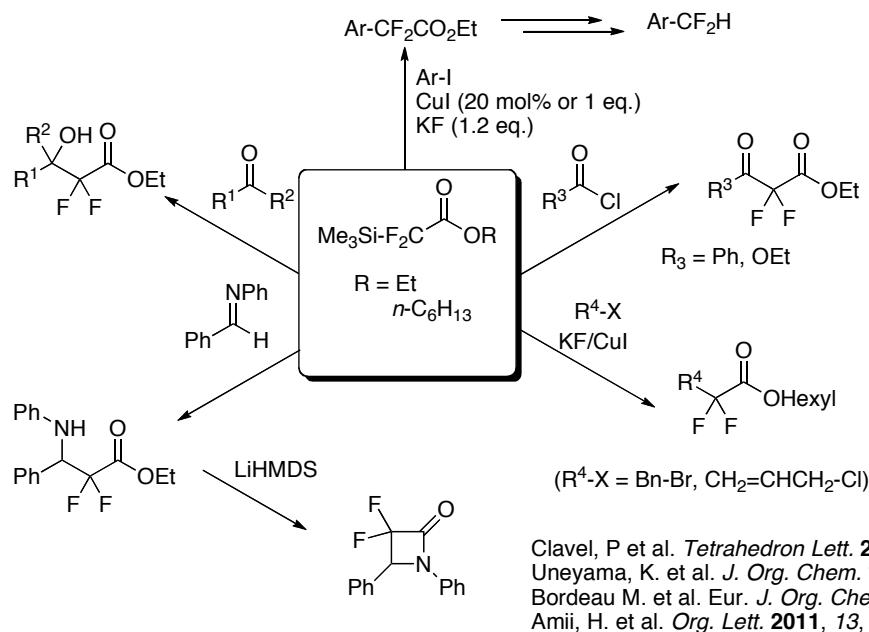
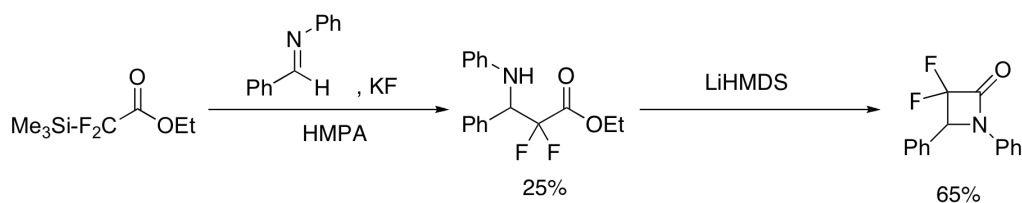


Figure 2-2. 2,2-Difluoro-2-(trimethylsilyl)acetates as a difluoromethylene building block

Nucleophilic addition of ethyl 2,2-difluoro-2-(trimethylsilyl)acetate to an imine followed by ring-closing reaction to give a difluoro β -lactam was reported (**Scheme 2-22**). However, only one example of nucleophilic addition to phenylidenebenzylamine was reported, to date. Reactions with other imines, for example, a reaction with benzylidenebenzylamine did not give desired adduct: The reaction gave ethyl difluoroacetate (the hydro-desilylated compound of 2,2-difluoro-2-(trimethylsilyl)acetate). Nucleophilic addition of 2,2-difluoro-2-(trimethylsilyl)acetates to imines has limitation in variation of imines.

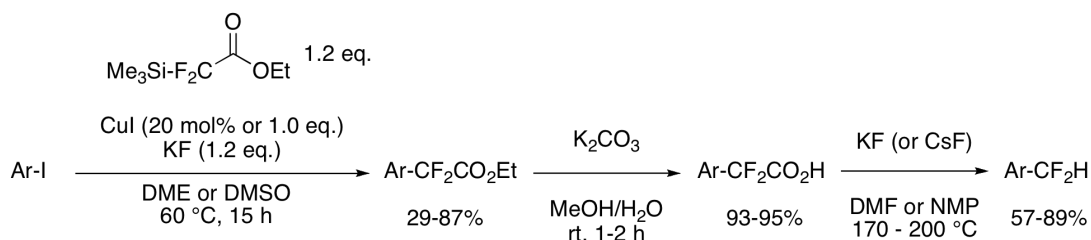


Bordeau, M.; Frébault, F. Gobet, M.; Picard, J.-P.
Eur. J. Org. Chem. **2006**, 4147–4154.

Scheme 2-22. Synthesis of difluoro β -lactams from ethyl 2,2-difluoro-2-(trimethylsilyl)acetate

Recently, Amii et al. have reported aromatic copper-catalyzed cross-coupling difluoromethylation

using ethyl 2,2-difluoro-2-(trimethylsilyl)acetate, copper-catalyzed cross-coupling followed by decarboxylation (**Scheme 2-23**) [25c]. Amii's group previously also developed a similar copper-catalyzed trifluoromethylation of aryl iodide using Ruppert-Prakash reagent ($\text{CF}_3\text{-SiMe}_3$ [26]) [27]. This study showed another synthetic possibility of $\text{Me}_3\text{Si-CF}_2\text{CO}_2\text{Et}$ like $\text{CF}_3\text{-SiMe}_3$.



Fujikawa, K.; Fujioka, Y.; Kobayashi, A.; Amii, H. *Org. Lett.* **2011**, *13*, 5560-5563.

Scheme 2-23. Difluoromethylation of aryl iodides with 2,2-difluoro-2-(trimethylsilyl)acetates

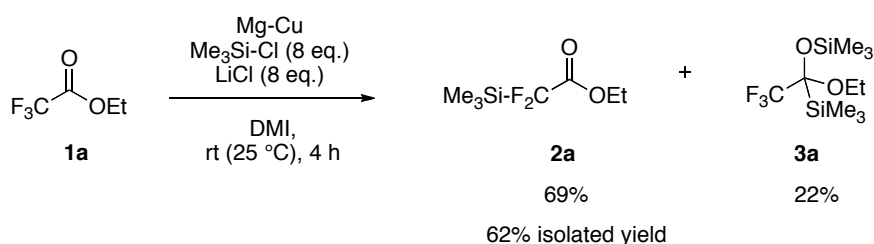
Advantages and disadvantages of a series of difluoromethylene building blocks were summarized in **Table 2-2**. Although the 2,2-difluoro-2-(trimethylsilyl)acetate has good properties as a reagent, it is less popular among these difluoromethylene building blocks. This situation is caused by the lack of efficient and practicable preparative method for 2,2-difluoro-2-(trimethylsilyl)acetates. In this chapter, reductive defluorination-silylation of readily available alkyl trifluoroacetates with Cu-deposited Mg metal as a reducing agent to give alkyl 2,2-difluoro-2-(trimethylsilyl)acetates, which is easy, inexpensive preparative method for alkyl 2,2-difluoro-2-(trimethylsilyl)acetates.

Table 2-2. Summary of α,α -difluoroacetate building blocks

CF ₂ CO ₂ R building blocks	Advantages	Disadvantages
	<ul style="list-style-type: none"> • A lot of reactions using BrCF₂CO₂Et have been developed. 	<ul style="list-style-type: none"> • relatively expensive (¥113,700/mol)
	<ul style="list-style-type: none"> • cheaper than BrCF₂CO₂Et 	<ul style="list-style-type: none"> • relatively expensive (¥45,700/mol) • reactions demand harsh conditions
	<ul style="list-style-type: none"> • applicable to asymmetric aldol reactions 	<ul style="list-style-type: none"> • moisture-sensitive • low yield from BrCF₂CO₂Et
 Ar = aryl moieties	<ul style="list-style-type: none"> • preparable via Mg(0)-reduction from CF₃CO₂Ar 	<ul style="list-style-type: none"> • preparable from moisture-sensitive CF₃CO₂Ar • moisture-sensitive
	<ul style="list-style-type: none"> • moisture-stable than difluoroketene silylacetate • preparable from ethyl trifluoromethylacetate, (cheap (¥19,900/mol) and moisture-stable) 	<ul style="list-style-type: none"> • No asymmetric reaction has been developed. • Only preparable methods via electrochemical reductions have been reported.

2-2. Results and discussion

Optimization of the reductive defluorination of ethyl trifluoroacetate (**1a**) by copper-deposited magnesium (Mg-Cu) in *N,N*-dimethylimidazolidinone (DMI) with LiCl as an additive gave ethyl 2,2-difluoro-2-(trimethylsilyl)acetate (**2a**) in 62% isolated yield (**Scheme 2-24**). The Cu-deposited Mg metal was prepared by mixing 4 molar equivalents of Mg powder and 0.5 molar equivalents of CuCl in a solution of LiCl in DMI just prior to the reaction. The silyl ketal byproduct, **3a**, [24c] was difficult to separate from **2a** by distillation because of a small difference in their boiling points. However, decomposing **3a** by adding anhydrous HCl/EtOH (prepared from Me₃Si-Cl and EtOH) enabled the isolation of **2a** by distillation. Details on the optimization of the reaction conditions are described below.



Scheme 2-24.

The effects of the transition metal deposits and the shape of the Mg metal are summarized in **Table 2-3**. The reaction without the addition of any transition metals resulted in recovery of ethyl trifluoroacetate, as was previously reported (entry 1). The Mg metal powder activated by FeCl₃ and NiCl₂ led to the decomposition of **1a** and gave the target compound **2a** in 1% and 2% yields, respectively (entries 3 and 4). The Mg metal activated by 0.25 molar equivalents of CuCl gave **2a** in 25% yield, and 48% of **1a** was recovered (entry 2). The use of 4 molar equivalents of the Mg metal powder activated by 0.5 molar equivalents of CuCl resulted in the complete consumption of **1a**. The reaction gave compounds **2a** and **3a** in a 50% and 45% yields, respectively (entry 5). The use of 4 molar equivalents of magnesium powder activated by 1.0 molar equivalents of CuCl resulted in the formation of the compound **2a** in 26% yield, and recovery of **1a** in 39% yield (entry 6). A mixture of Cu(0) powder and Mg metal powder reduced **1a** to **2a** in 3% yield (entry 7). These results suggest that “the Cu(0) powder attached on metallic Mg surface” is essential for efficient reduction of **1a**. The use of powdered Mg metal was also found to be essential. Magnesium turnings and magnesium ribbon resulted in lower conversions of the substrate (entries 8, 9, and 10). Use of commercially available Zn dust or Zn-Cu dust resulted in complete recoveries of the substrate **1a** (entries 11 and 12). Metallic Mg with a large surface area was necessary for the complete consumption of **1a** in the reaction.

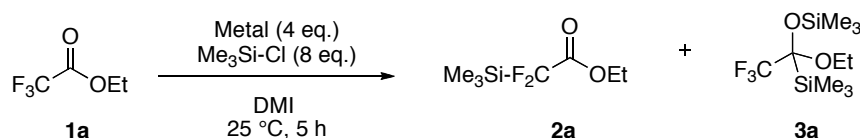


Table 2-3. Effects of metals on defluorination-silylation of ethyl trifluoroacetate (**1a**)

Entry	Metal reducing agent	Activation of Mg (eq.)	Recov. of 1a ^a [%]	Yields ^a (%)	
				2a	3a
1 ^b	Mg powder	-	100	0	0
2	Mg powder	CuCl (0.25)	48	(25)	(23)
3	Mg powder	FeCl ₃ (0.25)	84	(1)	(0)
4	Mg powder	NiCl ₂ (0.25)	38	(2)	(1)
5	Mg powder	CuCl (0.5)	0	(50)	(45)
6	Mg powder	CuCl (1.0)	39	(26)	(15)
7	Mg powder	Cu(0) (0.5) ^c	93	(3)	(2)
8	Mg turnings	CuCl (0.5)	70	(9)	(9)
9	Mg turnings ^d	CuCl (0.5)	44	(24)	(18)
10	Mg ribbon	CuCl (0.5)	45	(25)	(23)
11	Zn dust	-	100	0	0
12	Zn-Cu dust	-	100	0	0

^a Yields in parentheses and recoveries of **1a** were determined by ¹⁹F NMR with 4-(trifluoromethyl)anisole as an internal standard. ^b Reaction time is 24 hours. ^c Cu(0) powder was added to the suspension of Mg powder. ^d 12 Equivalent amounts of Mg turnings were used.

Results for the optimizations of reaction conditions by changing the solvent are summarized in **Table 2-4**. The use of the highly polar solvent DMF resulted in the formation of **2a** in 8% yield (entry 1). The use of DMI, whose dielectric constant is similar to that of DMF, resulted in the effective formation of the difluoroacetate **2a** in 50% yield (entry 2). The use of a similar cyclic amidic solvent, *N*-methylpyrrolidone (NMP), resulted in the formation of **2a** only in 14% yield (entry 3). The use of DMI/THF (1:9), THF, or acetonitrile resulted in the formation of the difluoroacetate **2a** only in 5% yield, 2% yield or 4% yield, respectively (entries 4, 5, and 6 respectively). Using DMI resulted in the highest yield among the solvents examined.

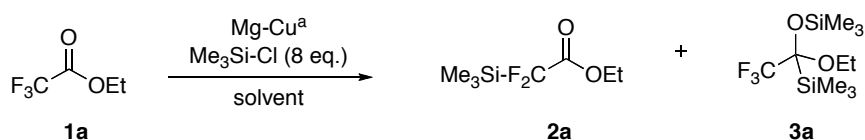


Table 2-4. Effects of solvent and temperature on defluorination-silylation of **1a**

Entry	Solvent	Temp.		Recov. of 1a ^b [%]	Yields ^b [%]	
		[°C]	Time [h]		2a	3a
1	DMF	25	5.0	70	(8)	(5)
2	DMI	25	5.0	0	(50)	(45)
3	NMP	25	5.0	36	(14)	(14)
4	DMI/THF (1:9)	25	24	78	(5)	(0)
5	THF	50	5.0	76	(2)	(0)
6	CH ₃ CN	25	5.0	86	(4)	(0)

^a Cu-deposited Mg metal was in situ prepared from Mg metal powder (4 eq.) and CuCl (0.5 eq.).

^b Yields in parentheses and recoveries of **1a** were determined by ¹⁹F NMR with 4-(trifluoromethyl)anisole as an internal standard.

Electrochemical reduction of **1a** gave compound **2a** in 68% yield by ¹⁹F NMR analysis of the crude mixture [24d], which was higher than the best reaction by conditions present in **Table 2-4** (entry 2, 50%). In order to determine if the electrolyte present in the electrochemical reaction was the reason for the higher yields, “supporting electrolyte” was added to the magnesium metal reaction. The results are summarized in **Table 2-5**. The reaction with Et₄NCl additive resulted in a lower conversion of **1a**. The reaction with an 8 equiv. amount of LiCl additive resulted in a 62% isolated yield (69% by ¹⁹F NMR analysis, entry 4). The reaction at 50 °C with 8 equiv. amount of LiCl resulted in lower yield (53%, entry 5). The reaction with 12 equiv. amount of LiCl resulted in the formation of **2a** in the same yield with the ketal **3a** in lower yield (20%; entry 6). Reactions with other lithium salt (LiBr (entry 7 and 8), LiClO₄ (entry 9), Li(OTf) (entry 10)) additives resulted in lower conversions of the substrate **1a** than that with LiCl (entry 4), although these additives suppressed the formation of the ketal **3a**. Other metal salt additives (MgBr₂·OEt₂ (entry 11 and 12) and KCl (entry 13)) did not suppress the formation of **3a**. Thus, the reaction in DMI with an 8 equiv. amount of LiCl was found to be the best

conditions for the preparation of **2a**, which was shown in **Scheme 2-24**.

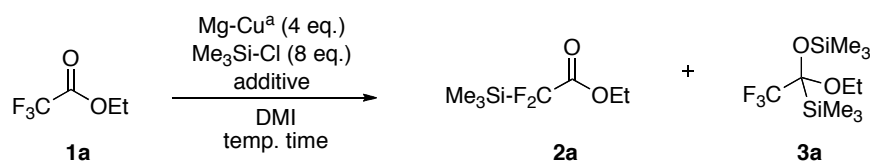
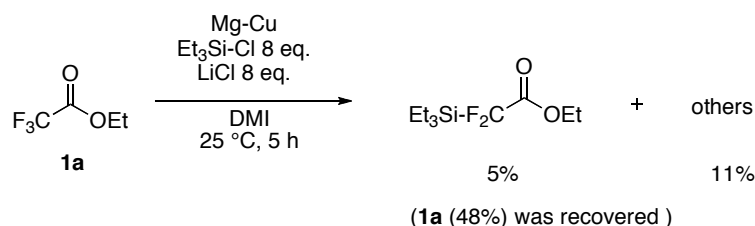


Table 2-5. Effects of additives on the defluorination-silylation reaction of **1a**

Entry	Additive (eq.)	Temp. [°C]	Time [h]	Recov. of 1a ^b [%]	Yields ^c [%]	
					2a	3a
1	-	25	5.0	0	(50)	(45)
2	Et ₄ NCl (16)	25	5.0	68	(18)	(14)
3	LiCl (4.0)	25	5.0	0	(62)	(26)
4	LiCl (8.0)	25	4.0	0	62 ^d (69)	(22)
5	LiCl (8.0)	50	3.0	0	(53)	(7)
6	LiCl (12)	25	5.0	2	(69)	(20)
7	LiBr (4.0)	25	5.0	56	(25)	(11)
8	LiBr (8.0) ^e	25	5.0	100	(0)	(0)
9	Li(ClO ₄) (4.0) ^e	25	5.0	100	(0)	(0)
10	Li(OTf) (4.0) ^e	25	5.0	95	(4)	(0)
11	MgBr ₂ ·OEt ₂ (0.5)	25	5.0	20	(43)	(34)
12	MgBr ₂ ·OEt ₂ (2.0) ^e	25	5.0	100	(0)	(0)
13	KCl (4)	25	5.0	59	(19)	(15)

^a Mg-Cu was in situ prepared from Mg powder (4 eq.) and CuCl (0.5 eq.). ^b Values were determined by ¹⁹F NMR of crude mixture containing solvent with 4-(trifluoromethyl)anisole as an internal standard. ^c Values in parentheses were yields determined by ¹⁹F NMR of crude mixture after extractions with benzotrifluoride as an internal standard. ^d The yield is the isolated yield. ^e The additives were not completely dissolved.

The defluorination–silylation reaction with another silylating agent, Et₃Si-Cl, resulted in low yield of difluoroacetate (5% yield determined by ¹⁹F NMR of the crude mixture, **Scheme 2-25**). This result suggested some contribution of silyl chlorides in rate-determining step of the reaction.



Scheme 2-25.

While variation in the silyl moiety led to reduced yields, variation in the alkyl moiety was successful; two primary (R = Et, *n*-C₆H₁₃) and two secondary (R = *i*-Pr, Cy) 2,2-difluoro-2-(trimethylsilyl)acetates **2a-d** were similarly produced from the corresponding trifluoroacetates under the optimized condition (Table 2-6). The *i*-propyl 2,2-difluoro-2-(trimethylsilyl)acetate **2c** was produced in 65% isolated yield using a similar procedure as that for **2a** (entry 3). The *n*-hexyl and the cyclohexyl 2,2-difluoro-2-(trimethylsilyl)acetates were isolated in 60% and 68% yields, respectively, by distillation followed after the decomposition of the silyl ketals **3b** and **3d** by reacting them with TFA (entries 2 and 4, respectively). The yields for products **2a-d** were comparable to those of electrochemical reductions [24d].

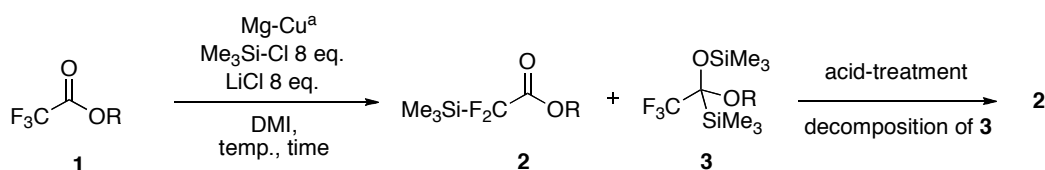
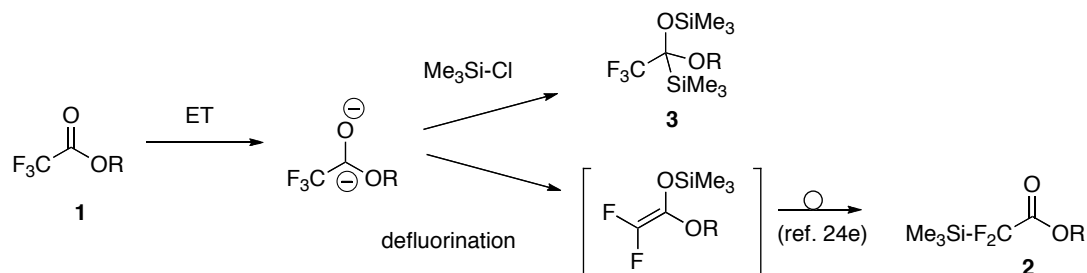


Table 2-6. Isolations of alkyl 2,2-difluoro-2-(trimethylsilyl)acetates (**2**)

Entry	R	Temp. (°C)	Time (h)	Conditions for acid-treatment	Yields ^c (%)		Ref 24d (2) ^d
					2 ^b	3	
1	Et (a)	rt (25)	4	Me ₃ Si-Cl (5 eq.)/EtOH, rt, 1 h	62 (69)	(22)	[47]
2	<i>n</i> -C ₆ H ₁₃ (b)	rt (25)	4	TFA (5 eq.), rt, 1 h	60 (68)	(24)	[62]
3	<i>i</i> -Pr (c)	rt (29)	3.5	Me ₃ Si-Cl (5 eq.), H ₂ O (2 eq.) / <i>i</i> -PrOH, rt, 10 h	65 (77)	(11)	-
4	Cy (d)	rt (23)	4	TFA (5 eq.), rt, 1 h	68 (73)	(18)	-

^aMg-Cu was in situ prepared from Mg powder (4 eq.) and CuCl (0.5 eq.). ^bIsolated yields by distillation after decomposition of silyl ketals **3** under acidic conditions (on 5 mmol scale). ^cValues in parentheses are yields in crude product mixture determined by ¹⁹F NMR with benzotrifluoride as an internal standard. ^dReported isolated yields by electrochemical reductions [ref 24d].

A plausible mechanism is illustrated in **Scheme 2-26**. Initial electron transfer(s) from Mg metal to the trifluoroacetates would give some anion species, followed by defluorination–silylation or double silylations [24c]. The enolate form of the product would be thermally rearranged to the ester **2** [24e].



Scheme 2-26. A plausible mechanism for the formation of **2** and the formation of **3**

2-3. Summary

In summary, alkyl 2,2-difluoro-2-(trimethylsilyl)acetates **2a-d** were produced by the reduction of alkyl trifluoroacetates **1** by copper-deposited magnesium, which can be easily prepared by the mixing of magnesium powder and CuCl in DMI with LiCl additive solution just prior to the reaction. Alkyl 2,2-difluoro-2-(trimethylsilyl)acetates **2** were isolated by distillation after the decomposition of byproducts **3** under acidic conditions.

In this study, the unsolved insight on the effect of addition of LiCl remains. Additional study on this item is described in appendix B of this thesis.

2-4. Experimental section

2-4-1. General

All NMR spectra were recorded as CDCl_3 solutions. ^1H NMR (600 MHz) was recorded with Varian Unity INOVA AS600. ^1H NMR (400 MHz), ^{13}C NMR (100 MHz), ^{19}F NMR (376 MHz) spectra were recorded with Varian VNMRS-400 instrument. The chemical shifts are reported in δ (ppm) related to the CHCl_3 (7.26 ppm for ^1H NMR), CDCl_3 (77 ppm for ^{13}C NMR) and C_6F_6 (0 ppm for ^{19}F NMR: The relative chemical shift of C_6F_6 to CFCl_3 is -162.2 ppm). Coupling constants (J) are reported in hertz (Hz). Infrared spectra were recorded on a Hitachi 270-30 spectrometer. Only selected absorbances are reported (ν in cm^{-1}). MS analyses were performed on a Shimadzu GCMS-QP5050A.

Elemental analyses were performed on a Perkin Elmer series II CHNS/O Analyzer 2400. Mg powder was purchased from Merck (particle size 0.1 mm, 97% pure, synthetic grade, catalog # 8.18506.0100). Copper(I) chloride was purchased from Wako pure chemicals (99.9% purity, catalog# 033-12482).

2-4-2. Procedures for reductions of alkyl trifluoroacetates (**1**) by Cu-deposited Mg and trimethylsilyl chloride

Synthesis of ethyl 2,2-difluoro-2-(trimethylsilyl)acetate (**2a**). Mg powder (0.486 g, 20 mmol), copper(I) chloride (0.248 g, 2.5 mmol), and anhydrous lithium chloride (1.7 g, 40 mmol) were stirred in DMI (10.0 ml) and Me₃Si-Cl (5.0 ml, 40 mmol) for 15 minutes under an argon atmosphere at room temperature. Ethyl trifluoroacetate (5 mmol, 0.71 g) was added dropwise into the stirred suspension. The suspension was stirred for additional 4 hours at room temperature. After removal of Cu-deposited Mg by decantation, the DMI solution was extracted with Et₂O. The Et₂O layer was washed with 10% HCl aq. and brine, dried over MgSO₄. Then, solvent was removed under a reduced pressure. The mixture of difluoro compound **2a** and silyl ketal **3a** was obtained.

Procedure for removal of **3a** from the mixture of **2a** and **3a**. Anhydrous HCl/EtOH was prepared from Me₃Si-Cl (3.0 ml, 25 mmol) and ethanol (2 ml, 34 mmol). The prepared anhydrous HCl/EtOH was added dropwise into the mixture of difluoro-compound **2a** and silyl ketal **3a**. After stirring 90 minutes at room temperature, the solution was extracted with ether (5 ml × 4). The combined organic layer was washed with brine. Organic layer was dried over MgSO₄, then, was concentrated under a reduced pressure. Kugelrohr distillation (100 °C/32 mmHg, bath temperature) of the crude product gave ethyl 2,2-difluoro-2-(trimethylsilyl)acetate (**2a**) in 62% (0.602 g) of isolated yield. Colorless oil. bp 70 °C/20 mmHg (bath temperature). IR ν_{\max} (neat) 2980, 1760 cm⁻¹. ¹H NMR (400 MHz, CDCl₃) δ 0.23 (s, 9H), 1.34 (t, *J* = 7 Hz, 3H), 4.31 (q, *J* = 7 Hz, 2H). [δ 0.16 (s, 9 H), 1.27 (t, *J* = 7 Hz, 3H), 4.24 (q, *J* = 7 Hz 2H). (ref. 24d)] ¹³C NMR (100 MHz, CDCl₃) δ -5.2 (s), 13.9 (s), 62.2 (s), 121.0 (t, *J* = 268 Hz), 166.3 (t, *J* = 26 Hz). ¹⁹F NMR (376 MHz, CDCl₃) δ 38.4 (s, 2F). [δ 38.7 (s, 2F). (ref. 24d)] EI-MS *m/z* (% relative intensity) 181 ([M]⁺-CH₃, 1), 153 (4), 117 (5), 73 (100).

Ethyl silyl ketal (**3a**). Compound **3a** was isolated from the reaction mixture with **2a** by column chromatography on silica gel (hexane eluent). Colorless oil. bp 80 °C/20 mmHg (bath temperature). IR ν_{\max} (neat) 2990, 2910 cm⁻¹. ¹H NMR (400 MHz, CDCl₃) δ 0.16 (q, *J* = 1 Hz, 9H), 0.17 (s, 9H), 1.19 (t, *J* = 7 Hz, 3H), 3.66 (m, 2H). [δ 0.18 (s, 9H), 0.19 (s, 9H), 1.21 (t, *J* = 7.0 Hz, 3H), 3.68 (m, 2H) (ref 24c)] ¹⁹F NMR (376 MHz, CDCl₃) δ 86.5 (s, 3F). [δ 86.7 (s, 3F). (ref 24c)] EI-MS *m/z* (% relative intensity) 259 ([M]⁺-C₂H₅, 6), 73 (100).

Synthesis of *n*-hexyl 2,2-difluoro-2-(trimethylsilyl)acetate (2b). The procedure to obtain the mixture of difluoro-compound **2b** and silyl ketal **3b** was similar to that of the mixture of **2a** and **3a**.

TFA (25 mmol, 2 ml) was added to the mixture of difluoro-compound **2b** and silyl ketal **3b**, and stirred additional 60 minutes at room temperature. The TFA solution of the crude mixture was extracted with *n*-hexane. The combined *n*-hexane solution was washed with 10% HCl aq. and brine. The *n*-hexane solution was dried over MgSO₄. After removal of the solvent under a reduced pressure, Kugelrohr distillation afforded *n*-hexyl 2,2-difluoro-2-trimethylsilylacetate (**2b**) in 60% (0.757 g) of isolated yield, respectively. Colorless oil. bp 90 °C/2 mmHg (bath temperature). IR ν_{\max} (neat) 2970, 1760 cm⁻¹. ¹H NMR (600 MHz, CDCl₃) δ 0.23 (s, 9H), 0.89 (t, *J* = 7 Hz, 3H), 1.28-1.34 (m, 4H), 1.34-1.40 (m, 2H), 1.69 (quint, *J* = 7 Hz, 2H), 4.24 (t, *J* = 7 Hz, 2H). [(200 MHz, CDCl₃) δ 0.23 (s, 9H), 0.89 (t, *J* = 6.6 Hz, 3H), 1.30-1.41 (m, 6H), 1.62-1.72 (m, 2H), 4.23 (t, *J* = 6.8 Hz, 2H). (ref 24d)] ¹⁹F NMR (376 MHz, CDCl₃) δ 38.4 (s, 2F). [δ 38.7 (s, 2F) (ref 24d)] EI-MS *m/z* (% relative intensity) 168 ([M]⁺-C₆H₁₂, 6), 152 (12), 77 (25), 73 (50), 43 (100).

***n*-Hexyl silyl ketal (3b).** Compound **3b** was isolated from the reaction mixture by column chromatography on silica gel (hexane eluent). 24% Yield (determined by ¹⁹F NMR). Colorless oil. bp 90 °C/2 mmHg (bath temperature). IR ν_{\max} (neat) 2970 cm⁻¹. ¹H NMR (400 MHz, CDCl₃) δ 0.16 (br, 9H), 0.17 (s, 9H), 0.89 (t, *J* = 7 Hz, 3H), 1.24-1.40 (m, 6H), 1.51-1.59 (m, 2H), 3.54-3.64 (m, 2H). ¹³C NMR (100 MHz, CDCl₃) δ -2.5 (s), 1.6 (s), 14.0 (s), 22.6 (s), 25.7 (s), 30.1 (s), 31.6 (s), 64.8 (s), 98.6 (q, *J* = 34 Hz), 124.9 (q, *J* = 288 Hz). ¹⁹F NMR (376 MHz, CDCl₃) δ 86.8 (s, 3F). EI-MS *m/z* (% relative intensity) 259 ([M]⁺-C₆H₁₃, 13), 73 (100). Elemental Anal. Calc for C₁₄H₃₁F₃O₂Si₂: C, 48.80; H, 9.07. Found: C, 48.86; H, 8.96.

Synthesis of *i*-propyl 2,2-difluoro-2-(trimethylsilyl)acetate (2c). The procedure to obtain the mixture of difluoro compound **2c** and silyl ketal **3c** was similar to that of the mixture of **2a** and **3a**.

Anhydrous HCl/*i*-PrOH was prepared from Me₃Si-Cl (25 mmol) and H₂O (0.18 ml, 10 mmol) and *i*-PrOH (2.6 ml, 34 mmol). The lower layer of the acidic mixture (*i*-PrOH layer) was added to the mixture of **2c** and **3c**, and stirred for additional 10 hours. The *i*-PrOH solution was extracted with Et₂O (5 ml × 5). The combined organic layer was washed with diluted HCl aq. and brine. Organic layer was dried over MgSO₄, and was concentrated under a reduced pressure. The mixture of the products was purified by Kugelrohr distillation (80 °C/20 mmHg, bath temperature), which provided isopropyl difluoro(trimethylsilyl)acetate **2c** in 65% (0.684 g) of isolated yield. Colorless oil. bp 80 °C/20 mmHg (bath temperature). IR ν_{\max} (neat) 2990, 1760 cm⁻¹. ¹H NMR (400 MHz, CDCl₃) δ 0.23 (s, 9H), 1.32 (d,

$J = 6$ Hz, 6H), 5.15 (sep, $J = 6$ Hz, 1H). ^{13}C NMR (100 MHz, CDCl_3) δ -5.2 (s), 21.4 (s), 70.1 (s), 120.8 (t, $J = 267$ Hz), 165.5 (t, $J = 25$ Hz). ^{19}F NMR (376 MHz, CDCl_3) δ 38.4 (s, 2F). EI-MS m/z (% relative intensity) 168 ($[\text{M}]^+ - \text{C}_3\text{H}_6$, 5), 153 (11), 117 (12), 77 (42), 73 (100). Elemental Anal. Calc for $\text{C}_8\text{H}_{16}\text{F}_2\text{O}_2\text{Si}$: C, 45.69; H, 7.67. Found: C, 45.80; H, 7.85.

Isopropyl silyl ketal (3c). Compound **3c** was isolated from the reaction mixture by column chromatography on silica gel (hexane eluent). 11% Yield (determined by ^{19}F NMR). Colorless oil. bp 85 °C/20 mmHg (bath temperature). IR ν_{max} (neat) 2990 cm^{-1} . ^1H NMR (400 MHz, CDCl_3) δ 0.13 (s, 9H), 0.18 (s, 9H), 1.13 (dd, $J = 16, 6$ Hz, 6H), 4.19 (sep(q), $J = 6$ Hz, 1H). ^{13}C NMR (100 MHz, CDCl_3) δ -3.2 (s), 1.8 (s), 23.3(s), 24.7 (s), 66.4 (s), 97.7 (q, $J = 34$ Hz), 125.1 (q, $J = 289$ Hz). ^{19}F NMR (376 MHz, CDCl_3) δ 87.4 (s, 3F). EI-MS m/z (% relative intensity) 259 ($[\text{M}]^+ - \text{C}_3\text{H}_7$, 7), 73 (100). Elemental Anal. Calc for $\text{C}_{11}\text{H}_{25}\text{F}_3\text{O}_2\text{Si}_2$: C, 43.68; H, 8.33. Found: C, 43.59; H, 8.28.

Synthesis of cyclohexyl 2,2-difluoro-2-(trimethylsilyl)acetate (2d). The procedure to obtain the mixture of difluoro compound **2d** and silyl ketal **3d** is similar to that of the mixture of **2a** and **3a**.

Procedure to remove **3d** from the mixture of **2d** and **3d** is the same to that of *n*-hexyl acetate **2b**. 68% Yield. Colorless oil. bp 90 °C/2 mmHg (bath temperature). IR ν_{max} (neat) 2950, 1750 cm^{-1} . ^1H NMR (600 MHz, CDCl_3) δ 0.23 (s, 9H), 1.29 (dtt, $J = 13, 10, 4$ Hz, 1H), 1.39 (dtt, $J = 14, 10, 4$ Hz, 2H), 1.48-1.52 (m, 2H), 1.55 (dtt, $J = 13, 8, 4$ Hz, 1H), 1.74-1.78 (m, 2H), 1.88-1.91 (m, 2H), 4.92 (tt, $J = 4, 10$ Hz, 1H). ^{13}C NMR (100 MHz, CDCl_3) δ -5.0 (s), 23.5 (s), 25.1 (s), 31.3 (s), 74.8 (s), 120.8 (t, $J = 267$ Hz), 165.6 (t, $J = 25$ Hz). ^{19}F NMR (376 MHz, CDCl_3) δ 38.6 (s, 2F). EI-MS m/z (% relative intensity) 168 ($[\text{M}]^+ - \text{C}_6\text{H}_{10}$, 14), 152 (19), 83 (74), 77 (31), 73 (57), 55 (100). Elemental Anal. Calc for $\text{C}_{11}\text{H}_{20}\text{F}_2\text{O}_2\text{Si}$: C, 52.77; H, 8.05. Found: C, 52.49; H, 8.31.

Cyclohexyl silyl ketal (3d). Compound **3d** was isolated from the reaction mixture by column chromatography on silica gel (hexane eluent). 18% Yield (determined by ^{19}F NMR). Colorless oil. bp 90 °C/2 mmHg (bath temperature). IR ν_{max} (neat) 2940, 2860 cm^{-1} . ^1H NMR (400 MHz, CDCl_3) δ 0.13 (br, 9H), 0.17 (s, 9H), 1.20-1.48 (m, 6H), 1.71-1.78 (m, 4H), 3.84-3.89 (m, 1H). ^{13}C NMR (100 MHz, CDCl_3) δ -3.1 (s), 1.8 (s), 24.0 (s), 24.3 (s), 25.7 (s), 33.3 (s), 34.7 (s), 71.7 (s), 97.7 (q, $J = 34$ Hz), 125.1 (q, $J = 289$ Hz). ^{19}F NMR (376 MHz, CDCl_3) δ 87.4 (s, 3F). EI-MS m/z (% relative intensity) 259 ($[\text{M}]^+ - \text{C}_6\text{H}_{11}$, 4), 147 (2), 73 (100). Elemental Anal. Calc for $\text{C}_{14}\text{H}_{29}\text{F}_3\text{O}_2\text{Si}_2$: C, 49.09; H, 8.53. Found: C, 48.98; H, 8.52.

2-5. References

- [1] (a) Tozer, M. J.; Herpinb, T. F. *Tetrahedron* **1996**, *52*, 8619-8683. (b) Welch, J. T.; Eswarakrishnan, S. *Fluorine in Bioorganic Chemistry*; John Wiley & Sons: New York, 1991.
- [2] (a) LaPlante, S. R.; Bonneau, P. R.; Aubry, N.; Cameron, D. R.; Déziel, R.; Grand-Maitre, C.; Plouffe, C.; Tong, L.; Kawai, S. H. *J. Am. Chem. Soc.* **1999**, *121*, 2974-2986. (b) Angelastro, M. R.; Baugh, L. E.; Bey, P.; Burkhart, J. P.; Chen, T-M.; Durham, S. L.; Hare, C. M.; Huber, E. W.; Janusz, M. J.; Koehl, J. R.; Marquart, A. L.; Mehdi, S.; Peet, N. P. *J. Med. Chem.* **1994**, *37*, 4538-4554. (c) Ogilvie, W.; Bailey, M.; Poupart, M-A.; Abraham, A.; Bhavsar, A.; Bonneau, P.; Bordeleau, J.; Bousquet, Y.; Chabot, C.; Duceppe, J-S.; Fazal, G.; Goulet, S.; Grand-Maitre, C.; Guse, I.; Halmos, T.; Lavallée, Leach, P. M.; Malenfant, E.; O'Meara, J.; Plante, R.; Plouffe, C.; Poirier, M.; Soucy, F.; Yoakim, C.; Déziel, R. *J. Med. Chem.* **1997**, *40*, 4113-4135. (d) Gelb, M. H.; Svaren, J. P.; Abeles, R. H. *Biochemistry* **1985**, *24*, 1813-1817. (e) Gelb, M. H. *J. Am. Chem. Soc.* **1986**, *108*, 3146-3147.
- [3] Sham, H. L. *Renin Inhibitors with Fluorine-containing Amino Acids*, In: *Fluorine-containing Amino Acids*; Kukahr, V.P.; Soloshonok, V. A.; Eds. John Wiley & Sons: Chichester, 1995; pp. 333.
- [4] (a) Schirlin, D.; Baltzer, S.; VanDorsselaer, V.; Weber, F.; Weill, C.; Altenburger, J. M.; Neises, B.; Flynn, G.; Rimy, J. M.; Tarnus, C. *Bioorg. Med. Chem. Lett.* **1993**, *3*, 253-258. (b) Welch, J. T. *Tetrahedron* **1987**, *43*, 3123-3197.
- [5] Caroline Doucet, C.; Isabelle Vergely, I.; Reboud-Ravaux, M.; Guilhem, J.; Kobaiter, R.; Joyeau, R.; Wakselman, M. *Tetrahedron: Asymmetry* **1997**, *8*, 739-751.
- [6] Joyeau, R.; Molines, H.; Labia, R.; Wakselman, M. *J. Med. Chem.* **1988**, *31*, 370-374.
- [7] (a) Uneyama, K.; Mizutani, G. Maeda, K.; Kato, T. *J. Org. Chem.* **1999**, *64*, 6717-6723. (b) Jonet, S.; Cherouvrier, F.; Brigaud, T. Portella, C. *J. Org. Chem.* **2005**, *70*, 4304-4312. (c) Jin, E.; Jiang, B.; Xu, Y. *Tetrahedron Lett.* **1992**, *33*, 1221. (d) Jin, E.; Xu, Y.; Huang, W. *J. Chem. Soc., Perkin Trans. I* **1993**, 795. (e) Fleming, I.; Roberts, R. S.; Smith, S. C. *J. Chem. Soc., Perkin Trans. I* **1998**, 1215. (f) Ichikawa, J.; Sonoda, T.; Kobayashi, H. *Tetrahedron Lett.* **1989**, *30*, 5437-5438.
- [8] (a) Sato, K.; Tarui, A.; Omote, M.; Ando, A.; Kumadaki, I. *Synthesis* **2010**, 1865-1882. (b) Ocampo, R.; Dolbier, W. R. Jr. *Tetrahedron* **2004**, *60*, 9325-9374. (c) Barma, D. K.; Kundu, A.; Zhang, H.; Mioskowski, C.; Falck, J. R. *J. Am. Chem. Soc.* **2003**, *125*, 3218-3219. For a method using PhSe-CF₂CO₂Et, see (d) Murakami, S.; Kim, S.; Ishii H.; Fuchigami, T. *Synlett* **2004**, 815-818.
- [9] Quan, H-D.; Tamura, M.; Gao, R.; Sekiya, A. *Tetrahedron* **2001**, *57*, 4111-4114.

- [10] For reviews, see (a) Lal, G. S.; Pez, G. P.; Syvret, R. G. *Chem. Rev.* **1996**, *96*, 1737-1755. (b) Banks, R. E.; Talow, J. C. In *Organofluorine Chemistry*; Banks, R. E., Smart, B. E., Tatlow, J. C., Eds: Plenum Press: New York, 1994; pp 42-44. (c) Chambers, R. D. *Fluorine in Organic Chemistry*; CRC Press LLC: Boca Raton, FL, 2004; pp 51-62. (d) Chambers, R. D.; Greenhall, M. P.; Hutchinson, J. *Tetrahedron* **1996**, *52*, 1-8. (e) Zajc, B.; Zupan, M. *J. Org. Chem.* **1982**, *47*, 573-575. (f) Inman, C. E.; Oesterling, R. E.; Tyczkowski, E. A. *J. Am. Chem. Soc.* **1958**, *80*, 6533-6535. (g) Xu, Z. Q.; DesMarteau, D. D.; Gotoh, Y. *Chem. Commun.* **1991**, 179-181. (h) Gupta, O. D.; Shreeve, J. M. *Tetrahedron Lett.* **2003**, *44*, 2799-2801. (i) Hagooley, A.; Sasson, R.; Rozen, S. *J. Org. Chem.* **2003**, *68*, 8287-8289. (j) Middleton, W. J.; Bingham, E. M. *J. Org. Chem.* **1980**, *45*, 2883-2887. (k) Tsushima, T.; Kawada, K.; Tsuji, T. *J. Org. Chem.* **1982**, *47*, 1107-1110. (l) Peng, W.; Shreeve, J. M. *J. Org. Chem.* **2005**, *70*, 5760-5763. (m) Loghmani-Khouzani, H.; Poorhervi, M. R.; Sadeghi, M. M. M.; Caggiano, L.; Jackson, R. F.W. *Tetrahedron* **2008**, *64*, 7419-7425.
- [11] Kitazume, T.; Ohnogi, T.; Lin, J. T.; Yamazaki, T. *J. Fluorine Chem.* **1989**, *42*, 17-29.
- [12] Sato, S. et al. Japan Patent Kokai 1999-80084.
- [13] (a) Hallinan, E. A.; Fried, J. *Tetrahedron Lett.* **1984**, *25*, 2301-2302. (b) Lang, E.W.; Schaub, B. *Tetrahedron Lett.* **1988**, *29*, 2943-2946. (c) Cheguillaume, A.; Lacroix, S.; Jacqueline Marchand-Brynaert, J. *Tetrahedron Lett.* **2003**, *44*, 2375-2377. (d) Sorochinsky, A.; Voloshin, N.; Markovsky, A.; Belik, M.; Yasuda, N.; Uekusa, H.; Ono, T.; Berbasov, D. O.; Soloshonok, V. A. *J. Org. Chem.* **2003**, *68*, 7448-7454.
- [14] (a) Ocampo, R.; Dolbier, W. R. Jr. *Tetrahedron* **2004**, *60*, 9325-9374. (b) Ashwood, M. S.; Cottrell, I. F.; Cowden, C. J.; Wallace, D. J.; Davies, A. J.; Kennedy, D. J.; Dolling, U. H. *Tetrahedron Lett.* **2002**, *43*, 9271-9273.
- [15] Sato, K.; Omote, M.; Ando, A.; Kumadaki, I. *J. Fluorine Chem.* **2004**, *125*, 509-515.
- [16] Inoue, M.; Araki, K. Kokai Tokkyo Koho, 2010-116363.
- [17] (a) Tarui, A.; Ozaki, D.; Nakajima, N.; Yokota, Y.; Sokeirek, Y. S.; Sato, K.; Omote, M.; Kumadaki, I.; Ando, A. *Tetrahedron Lett.* **2008**, *49*, 3839-3843. For a review, see (b) Tarui, A.; Sato, K.; Omote, M.; Kumadaki, I.; Ando, A. *Adv. Synth. Catal.* **2010**, *352*, 2733-2744.
- [18] (a) Kumai, K.; Seki, T. Japan Patent Kokai 1994-239792. (b) Brown, M. et al. Japan Patent Kokai 1999-92423.
- [19] Lang, R. W.; Schaub, B. *Tetrahedron Lett.* **1988**, *29*, 2943-2946.
- [20] Yoshida, M. Suzuki, D.; Iyoda, M. *J. Chem. Soc., Perkin Trans. 1* **1997**, 643-648.
- [21] (a) Huang, X-T.; Long, Z-Y. Chen, Q-Y. *J. Fluorine Chem.* **2001**, *111*, 107-113. (b) Ghattas, W.; Hess, C. R.; Icazio, G.; Hardr, R.; Klinman, J. P.; Réglie M. *J. Org. Chem.* **2006**, *71*,

- 8618-8621.
- [22] Iseki, K.; Kuroki, Y.; Asada, D.; Takahashi, M.; Kishimoto S.; Kobayashi, Y. *Tetrahedron* **1997**, *53*, 10271-10280.
- [23] (a) Iseki, K.; Kuroki, Y.; Asada, D.; Kobayashi, Y. *Tetrahedron Lett.* **1997**, *38*, 1447. (b) Iseki, K.; Kuroki, Y.; Asada, D.; Takahashi, M.; Kishimoto, S.; Kobayashi, Y. *Tetrahedron* **1997**, *53*, 10271-10280. (c) Iseki, K. *Tetrahedron* **1998**, *54*, 13887. (d) Poulain, F.; Serre, A-L.; Lalot, J.; Leclerc, E; Quirion, J-C. *J. Org. Chem.* **2008**, *73*, 2435-2438.
- [24] (a) Stepanov, A. A.; Minyaeva, T. V.; Martynov, B. I. *Tetrahedron Lett.* **1999**, *40*, 2203-2204. (b) Clavel, P.; Biran, C.; Bordeau, M.; Roques, N.; Trévin, S. *Tetrahedron Lett.* **2000**, *41*, 8763-8767. (c) Bordeau, M.; Clavel, P.; Barba, A.; Berlande, M.; Biran, C.; Roques, N. *Tetrahedron Lett.* **2003**, *44*, 3741-3744. (d) Uneyama, K.; Mizutani, G. *Chem. Commun.* **1999**, 613–614. (e) Uneyama, K.; Mizutani, G.; Maeda, K.; Kato, T. *J. Org. Chem.* **1999**, *64*, 6717-6723. (f) Amii, H. Kobayashi, T.; Uneyama, K. *Synthesis* **2000**, 2001-2003.
- [25] (a) Kawano, Y.; Kaneko, N.; Mukaiyama, T. *Bull. Chem. Soc. Jpn.* **2006**, *79*, 1133-1145. (b) Bordeau, M.; Frébault, F. Gobet, M.; Picard, J.-P. *Eur. J. Org. Chem.* **2006**, 4147-4154. (c) Fujikawa, K.; Fujioka, Y.; Kobayashi, A.; Amii, H. *Org. Lett.* **2011**, *13*, 5560-5563.
- [26] For preparation of CF_3SiMe_3 , see (a) Ruppert, I.; Schlich, K.; Volbach, W. *Tetrahedron Lett.* **1984**, *25*, 2195-2198. Reactions with KF/CuI system, see (b) Urata, N.; Fuchikami, T. *Tetrahedron Lett.* **1991**, *32*, 91-94. (c) Dubinina, G. G.; Furutachi, H.; Vicic, D. A. *J. Am. Chem. Soc.* **2008**, *130*, 8600-8601. For nucleophilic additions of CF_3SiMe_3 into various electrophiles, see (d) Prakash, G. K. S.; Krishnamurti, R.; Olah, G. A. *J. Am. Chem. Soc.* **1989**, *111*, 393-395. (e) Ramaiah, P.; Krishnamurti, R.; Prakash, G. K. S. *Org. Synth.* **1995**, *72*, 232-240. (f) Krishnamurti, R.; Bellew, D. R.; Prakash, G. K. S. *J. Org. Chem.* **1991**, *56*, 984-989.
- [27] Oishi, M.; Kondo, H.; Amii, H. *Chem. Commun.* **2009**, 1909–1911.

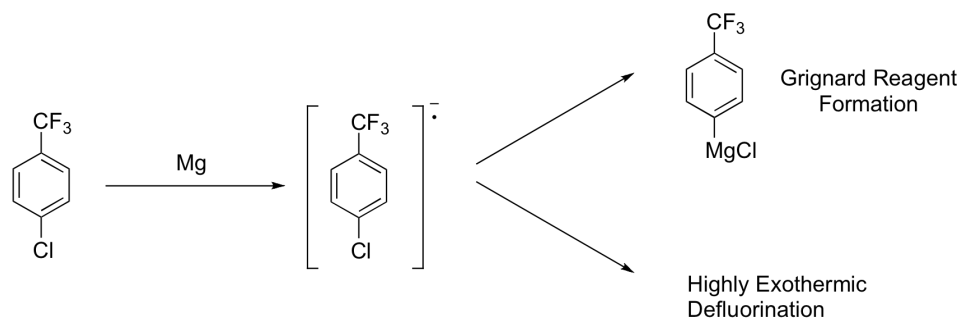
Chapter 3. Control of reductive benzylic defluorinations of (pentafluoroethyl)halobenzenes with use of Cu-deposited Mg metal

3-1. Introduction

3-1-1. Hazard in preparations of perfluoroalkylated aryl Grignard reagents

Preparations of (trifluoromethyl)phenylmagnesium halides (*m*- and *p*-CF₃-C₆H₄-MgX) are hazardous for its risk of explosion [1, 6]. For example, an accidental runaway reaction during the preparation of 4-(trifluoromethyl)phenylmagnesium chloride on a commercial scale resulted in loss of life and destruction of a chemical plant [1a]. For another example, severe decomposition during the formation of 3-trifluoromethylphenylmagnesium bromide causing extensive damage to a laboratory was reported [1b]. This important safety issue has hindered the use of trifluoromethyl-substituted phenyl Grignard reagents in large-scale organic synthesis, although (trifluoromethyl)phenyl moieties are frequently encountered in pharmaceutical drugs [2], catalysts [3], and synthetic intermediates [4].

The runaway reactions have been attributed to the highly exothermic Mg-F bond formations in defluorinations promoted by magnesium reduction (**Scheme 3-1**). Ashby et al. have supposed CF₃ group itself can react with magnesium when magnesium is sufficiently activated, like the reactions of benzotrichloride or benzotribromide [1c]. The hazard in formation of (trifluoromethyl)phenyl Grignard reagents has necessitated a method to suppress the defluorination process.

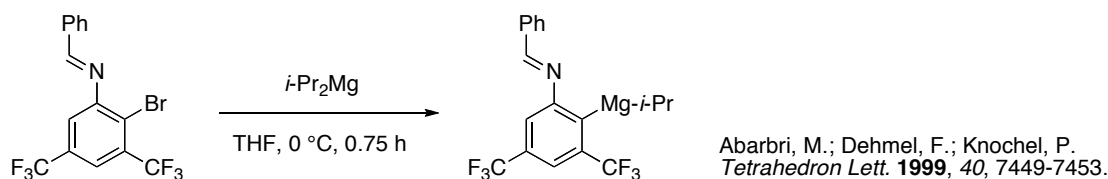


Scheme 3-1. Processes in reduction of 4-chlorobenzotrifluoride

3-1-2. Studies to prevent runaway reactions in Grignard reagent formation from perfluoroalkylated aryl halides

Several studies to prevent runaway reactions in Grignard reagent formation from perfluoroalkylated aryl halides have been reported.

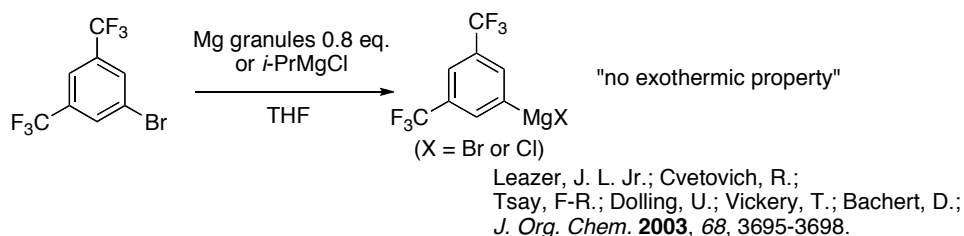
Grignard reagent formation via halogen-metal-exchange reaction of aromatic Br atom with *i*-Pr₂Mg (or *i*-PrMgCl) from a substrate bearing two trifluoromethyl groups at 0 °C was reported by Knochel et al. (**Scheme 3-2**), although there is no mentions on safety of the Grignard reagent formation in the report [5]. This method enables the Grignard reagent formation below 0 °C. From the safety point of view, this Knochel's methodology would seem to possess attractive characteristics for large-scale preparation.



Scheme 3-2. A Knochel's protocol for Br-Mg-exchange reaction at 0 °C

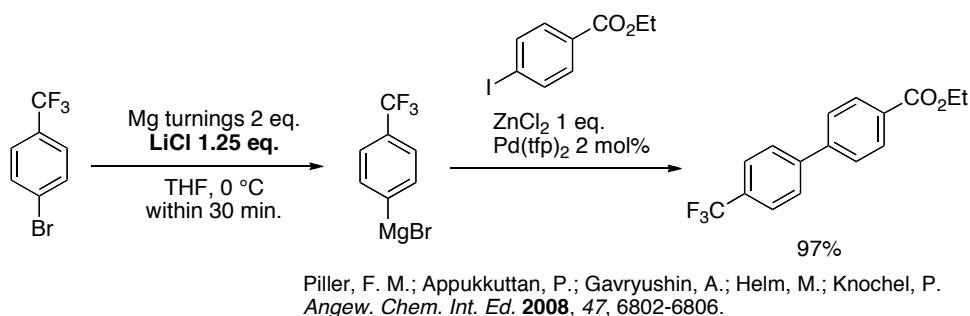
Safety analyses of preparations of 3,5-bis(trifluoromethyl)phenyl Grignard reagent from corresponding bromide with “Differential Thermal Analysis (DTA)” and “Reactive System Screening Tool (RSST)” were reported by Leather et al. (**Scheme 3-3**) [6a]. The 3,5-bis(trifluoromethyl)phenyl Grignard reagent prepared by Knochel's protocol, the Grignard reagent prepared by traditional preparation using 0.8 equivalent amounts of Mg metal granules, and the Grignard reagent after removal of residual Mg metal were analyzed by DTA and RSST. As results, these Grignard reagent preparations indicated no exothermic properties. Only Grignard reagent in the presence of residual excess Mg metal indicated exothermic property. In their conclusion, detonations associated with

formation of (trifluoromethyl)phenyl Grignard reagents may be attributed to loss of contact with solvent, runaway exothermic side reactions, and the presence of a highly activated form of metallic Mg. In the report, 3,5-bis(trifluoromethyl)phenyl Grignard reagent was reproducibly prepared without detonations by carefully controlling these factors. It also be concluded that Knochel's protocol is safer procedure than the method using metallic Mg. Although their study has revealed the factors of detonations, their study is not sufficient to prepare (trifluoromethyl)phenyl Grignard reagents safely, because the method to suppress defluorination reactions itself has not been developed.



Scheme 3-3. Leazer's protocol for preparation of 3,5-bis(trifluoromethyl)phenyl Grignard reagent

Knochel has reported the formation of 4-(trifluoromethyl)phenylmagnesium bromide by Mg activated by LiCl (**Scheme 3-4**) [6d]. The use of magnesium turnings in the presence of LiCl led to a safe magnesium insertion into 4-bromobenzotrifluoride at 0 °C and produced the Grignard reagent within 30 minutes. The method using LiCl does not need to use *i*-PrMgBr, that is, there is no chance to contaminate residual *i*-PrMgBr.



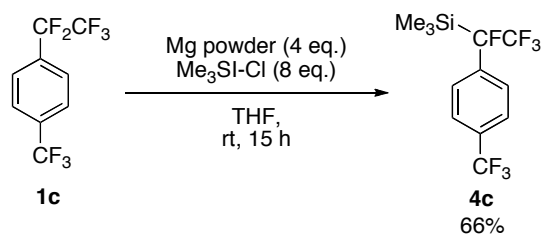
Scheme 3-4. Knochel's protocol for preparation of 4-(trifluoromethyl)phenylmagnesium bromide

As a result of their reports, control of temperature, removal of highly activated Mg metal, and loss of contact to solvent are methods to suppress the runaway reactions. However, these methods need careful control of the reactions. Another direct approach to suppress defluorinations will make the preparations of (trifluoromethyl)phenyl Grignard reagents more safe.

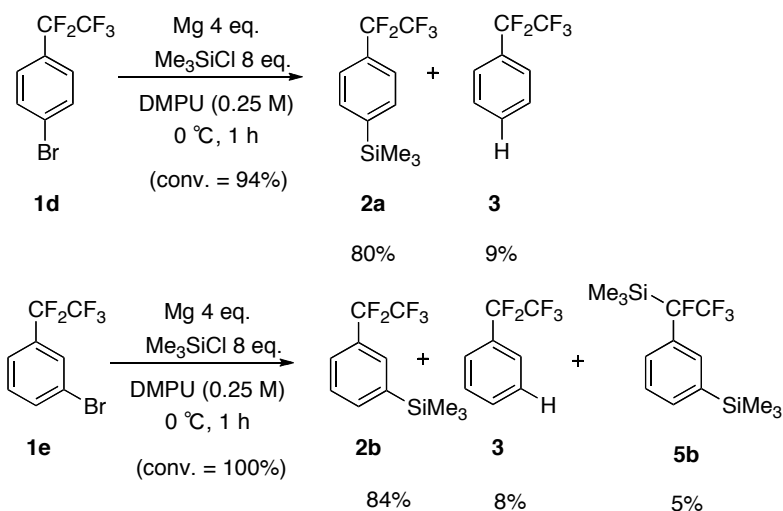
3-2. Results and discussion

3-2-1. Optimization of reaction conditions

I encountered a similar problem during our study of the reductive defluorination [7] of 1-chloro-4-(pentafluoroethyl)benzene (**1a**) with metallic Mg powder and Me₃Si-Cl [7f]. Reductive reaction of **1a** by powdered metallic Mg in 1,3-dimethyl-3,4,5,6-tetrahydro-2(1*H*)-pyrimidinone (DMPU) in the presence of Me₃Si-Cl gave ring-silylated compound **2a** and defluorinated compound **4a** simultaneously (Table 3-1, entry 1). In this study, the defluorination of the benzylic fluorine of the pentafluoroethyl group was found to be easier than that of the trifluoromethyl group (Scheme 3-5). Moreover, Grignard reagent formation from aryl chloride is more difficult than that from the bromide (Scheme 3-6). Thus, the reaction of compound **1a** with Mg/Me₃Si-Cl could be a model reaction to find the conditions for the suppression of defluorination.



Scheme 3-5. Reductive defluorination-silylation of 1-trifluoromethyl-4-(pentafluoroethyl)benzene (**1c**)



Scheme 3-6. Reductive reactions of bromo-substituted (pentafluoroethyl)benzenes using metallic Mg and Me₃Si-Cl.

Solvent screening was performed (Table 3-1). Two ureal solvents (DMPU and DMI), three amidic solvents, two ethereal solvents, and acetonitrile and toluene were used as dried solvents. Use of the ureal or amidic solvents gave compound **4a** as the main product (entries 1 - 5). Use of less polar solvents, THF, diethyl ether and toluene resulted in complete recovery of starting material (entries 6, 7, and 8, respectively). This lack of reaction in THF could be caused by a lack of self-catalytic action of the Grignard reagent species. Use of acetonitrile also resulted in complete recovery of **1a**, despite of its high dielectric constant (entry 9). This result may be attributed to low Gutmann's donor number (DN) of the acetonitrile (DN = 14.1) [8a]. These results indicate that the higher DN of the solvent is, the higher conversions of **1a** become, which suggests that the driving force of the reaction is dissociation of metallic Mg species into the solvent, not the stabilization of the anion species.

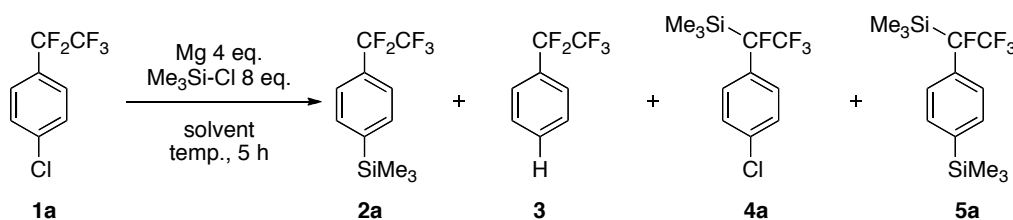


Table 3-1. Solvent effect in the reductive reaction of **1a** using metallic Mg

entry	solvent	Properties of the solvent			temp. [°C]	conv. of 1a ^a [%]	Yields ^a [%]				
		dielectric constant ϵ	DN ^b	AN ^c			2a	3	4a	5a	total
1	DMPU	36.12	(27) ^e	(16) ^e	0	100	22	5	44	5	87
2	DMI	37.60	(27) ^e	(19) ^e	0	100	9	6	42	24	82
3	DMA ^d	37.80	27.8	13.6	0	100	13	14	54	18	99
4	NMP	32.2	27.3	13.3	0	100	20	12	54	16	100
5	DMF	38.0	26.6	16	0	82	24	4	32	1	93
6	THF	7.6	20	8	55	0	0	0	0	0	0
7	Et ₂ O	4.34	19.2	3.9	reflux	0	0	0	0	0	0
8	toluene	2.38	Unknown	Unknown	55	0	0	0	0	0	0
9	CH ₃ CN	37.5	14.1	18.9	55	0	0	0	0	0	0

^a Yields and conversions of **1a** were determined by ¹⁹F NMR with benzotrifluoride as an internal standard. ^b DN_s stand for Gutmann's donor numbers, which indicate Lewis basicity of the solvents. ^c AN_s stand for Gutmann's acceptor numbers, which indicate Lewis acidity of the solvents. ^d DMA = Dimethylacetamide. ^e DN_s and AN_s in parentheses were estimated according to [ref. 8b] and [ref. 8c], respectively.

The recovery of the compound **1a** of the reaction in THF (entry 6) indicated that no initial electron transfer from metallic Mg to compound **1a** occurred. However, THF has been considered to be appropriate solvent to form Grignard reagents, even from aryl chlorides [1d]. Metallic Mg activated by a variety of metal salts were used in the same conditions (**Table 3-2**). Addition of alkali metal salts or alkaline earth metal salts including LiCl resulted in recovery of **1a**. Meanwhile, activation by transition metal gave the product **2a** (or **3**) as a main product. Particularly, activation by TiCl₃, FeCl₃, CoCl₂, MnCl₂, CuCl₂, and CuCl gave better conversion and better selectivity for **2a** (entries 18, 17, 16, 15, 14, and 13) than the reactions using pure metallic Mg in ureal or amidic solvents in **Table 3-1**. Here, conventional activation of metallic Mg such as addition of iodine, 1,2-bromoethane, and sonication during the reaction resulted in recovery of **1a**. These results suggested this better selectivity

for compound **2a** is attributed to the use of less polar solvent and/or activations of metallic Mg by transition metal salts.

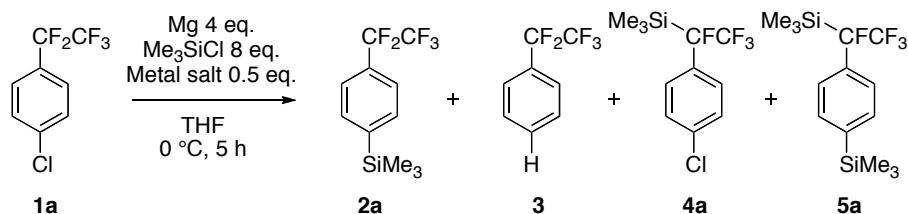


Table 3-2. Effects of metal salt additives

entry	Metal salt ^a	conv. [%] ^b	¹⁹ F NMR Yield ^b [%]					total ^c	entry	Metal salt ^a	conv. [%] ^b	¹⁹ F NMR Yield ^b [%]					total ^c
			2a	3	4a	5a	total ^c					2a	3	4a	5a	total ^c	
1	none	0	0	0	0	0	100	10	SnCl ₄	33	12	4	5	0	97		
2	KCl	0	0	0	0	0	100	11	NiCl ₂	24	10	12	4	0	93		
3	LiCl	0	0	0	0	0	100	12	SnCl ₂	55	35	5	20	0	105		
4	AlCl ₃	0	0	0	0	0	100	13	CuCl	48	25	5	13	0	95		
5	PdCl ₂	0	0	0	0	0	96	14	CuCl ₂	65	34	8	20	0	98		
6	ZrCl ₄	0	0	0	0	0	100	15	MnCl ₂	78	48	9	22	0	104		
7	CeCl ₃	0	0	0	0	0	100	16	CoCl ₂	100	28	29	21	2	89		
8	BF ₃ OEt ₂	0	0	0	0	0	96	17	FeCl ₃	100	36	13	28	26	103		
9	ZnCl ₂	5	2	0	1	0	96	18	TiCl ₃	100	19	5	30	39	82		

^a Mg powder (4.0 equiv.) was mixed with metal salts (0.5 equiv.) in THF for 15 minutes just prior to the reactions.

^b Yields and conversions of **1a** were determined by ¹⁹F NMR with benzotrifluoride as an internal standard. ^c The “total” stands for mass balance on ¹⁹F NMR.

To determine whether the better selectivity for **2a** is attributed to the less polar solvent or not, the use of further less polar solvents, mixed solvent of THF and Et₂O were examined, with effective activation of metallic Mg by transition-metal salts shown in **Table 3-3**. The selectivities for **2a** were compared to the ratio of Et₂O in the solvent (entries 11-18). As a result, the reaction in THF-Et₂O (1:9) with metallic Mg activated by CuCl (Cu-deposited Mg metal) gave compound **2a** in good yield (entry 17). The reaction in THF-Et₂O solvent with metallic Mg activated by FeCl₃ gave by-products and gave compound **2a** in lower yield. Use of Cu-deposited Mg metal gave good conversion of

substrates and less formation of by-products than use of FeCl₃-activated Mg metal or CoCl₂-activated Mg metal. Furthermore, the formation of **2a**, defluorination reaction, was avoided by the use of less polar solvent.

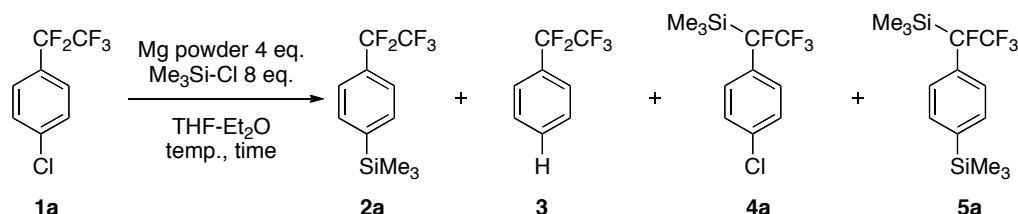


Table 3-3. Effects of Lewis acids in THF-Et₂O mixed solvents

Entry	Activation of Mg (eq.) ^a	Solvent		Temp. [°C]	Time [h]	Conv. of 1a ^b [%]	¹⁹ F NMR Yields ^b [%]			
		THF [v%]	Et ₂ O [v%]				2a	3	4a	5a
1	FeCl ₃ (0.1)	100	0	0	5	99	49	7	30	6
2	"	50	50	rt	5	89	47	23	13	5
3	"	25	75	rt	5	100	39	22	2	6
4	"	17	83	rt	5	88	35	29	1	0
5	"	0	100	40	10	0	0	0	0	0
6	TiCl ₃ (0.5)	100	0	rt	5	100	19	5	30	39
7	TiCl ₃ (0.1)	100	0	rt	15	0	0	0	0	0
8	CoCl ₂ (0.1)	100	0	0	0	51	27	4	17	1
9	"	25	75	30	5	100	39	22	0	6
10	"	0	100	40	5	0	0	0	0	0
11	CuCl (0.1)	100	0	0	5	10	4	4	2	0
12	"	33	67	rt	5	83	47	17	6	1
13	"	0	100	0	10	0	0	0	0	0
14	CuCl (0.5)	100	0	0	5	38	25	5	13	0
15	"	50	50	30	1.5	100	66	7	0	14
16	"	25	75	30	1.5	100	90	6	0	3
17	"	10	90	30	24	94	69	12	0	0
18	"	0	100	30	1.5	0	0	0	0	0

^a Mg powder (4.0 equiv.) was mixed with metal salts (0.5 equiv.) in THF for 15 minutes. ^b Yields and conversions of **1a** were determined by ¹⁹F NMR with benzotrifluoride as an internal standard.

The reproducibilities of the reactions of **1a** were examined (**Table 3-3**), because the reactions using metal reducing agents are often accompanied by induction periods. The same experiments were

induction period at the first stage of the reaction of 3 of 5 experiments (runs 7, 8, and 10). So long as our trials, CuCl and CuBr are less soluble in Et₂O than in THF. From that reason, the reaction in Et₂O using in situ generated Cu-deposited Mg metal resulted in very slow reactions or long induction periods. Thus, a minimum amount of THF was necessary to form Cu deposits on metallic Mg surfaces effectively.

The solvent effect on the product distribution in **Table 3-4** and **Table 3-5** is consistent with the conventional “diffusion mechanism of the Grignard reagent formation” (**Figure 3-1**). The diffusion mechanism suggests that anion radicals on the surface of the metallic Mg are converted into the Grignard reagent, whereas those far above the surface are converted into side products, such as homocoupling products. In the present case, a less polar solvent prevented long-distance electron transfer and/or the diffusion of anion radical species from the Mg metal surface by destabilizing the negative charges. The occurrence of the concerted electron transfer and C-Cl bond cleavage processes only at the surface would promote the predominant formation of the Grignard reagents, which would be followed by the transmetalation to yield the ring silylated product **2**. In contrast, a highly polar solvent would promote diffusion of the anion radical species far away from the metallic Mg surface. The “solvent-caged” anion radical species would lead to defluorinated product **4** due to π^* - σ^* negative hyperconjugation.

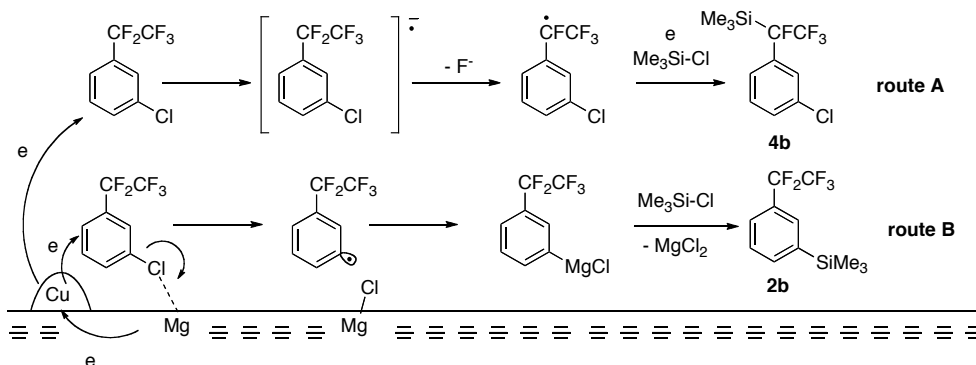


Figure 3-1. Plausible mechanisms for defluorination-silylation (route A), and Grignard reagent formation (route B).

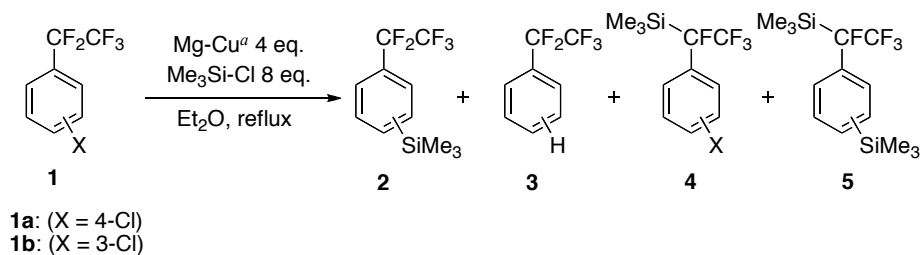


Table 3-6. Experimental data for the reactions in Et₂O in **Table 3-4** and **Table 3-5**

Run	Substrate 1	Time [h]	Conv. [%]	Yields ^b [%]			
				2	3	4	5
1	1a (X = 4-Cl)	5	10	3	6	0	0
	"	24	50	14	20	0	0
2	1a (X = 4-Cl)	5	11	2	4	0	0
	"	24	56	25	16	0	0
3	1a (X = 4-Cl)	5	0	0	0	0	0
	"	24	17	9	8	0	0
4	1a (X = 4-Cl)	5	18	7	9	0	0
	"	24	66	29	27	0	0
5	1a (X = 4-Cl)	5	0	0	0	0	0
	"	24	24	4	4	0	0
6	1b (X = 3-Cl)	5	0	0	0	0	0
	"	24	0	0	0	0	0
7	1b (X = 3-Cl)	1.5	0	0	0	0	0
	"	5	78	35	26	0	0
8	1b (X = 3-Cl)	5	0	0	0	0	0
	"	24	67	25	27	0	0
9	1b (X = 3-Cl)	5	0	0	0	0	0
	"	24	0	0	0	0	0
10	1b (X = 3-Cl)	5	0	0	0	0	0
	"	24	64	31	26	0	0
11	1b (X = 3-Cl)	5	0	0	0	0	0
	"	24	0	0	0	0	0

^a Mg-Cu was in situ generated from Mg powder (4 equiv.) and CuBr (0.5 equiv.) in Et₂O. ^b Yields were determined by ¹⁹F NMR with benzotrifluoride as an internal standard.

Finally, the optimized condition was applied to the Grignard reagent formation from bromobenzotrifluorides (**Table 3-7**). The yields of adducts of Grignard reactions of the (trifluoromethyl)phenylmagnesium bromides which were generated under the conventional and the improved conditions, to benzophenone were compared [10]. As results, the yields of adducts in the improved condition were comparable to those in conventional conditions. These results showed that Cu-deposited Mg does not result in lower yields of these Grignard reagents. Thus, the improved

condition would be applicable to the Grignard reagent formations of these halo-benzotrifluorides.

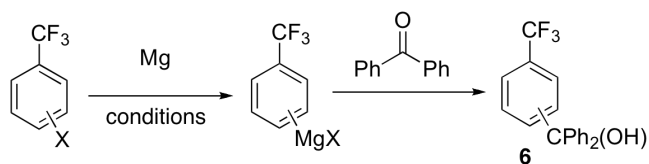


Table 3-7. Grignard reagent formations and Grignard reactions from 3- or 4-bromobenzotrifluoride

entry	X	Conditions ^a	Isolated yields of 6 [%]
1	4-Br (a)	Mg turnings (1.2 eq.), THF (1.0 M)	74 (6a)
2	4-Br (a)	Mg powder (1.2 eq.), CuCl (10 mol%), THF/Et ₂ O (1:3, 0.25 M)	79 (6a)
3	3-Br (b)	Mg turnings (1.2 eq.), THF (1.0 M)	83 (6b)
4	3-Br (b)	Mg powder (1.2 eq.), CuCl (10 mol%), THF/Et ₂ O (1:3, 0.25 M)	82 (6b)

^a Reactions were performed on 3 mmol scales.

3-2-2. Observations of Cu-deposited Mg surface

The surface of the Cu-deposited Mg metal was observed with a microscope to make the working hypothesis shown in **Figure 3-1** more certain. If the working hypothesis is correct, Mg(0) atoms near the Cu(0) deposits must be consumed. The surfaces of Cu-deposited Mg metal after the reactions were performed to observe whether Mg(0) atoms only near the Cu(0)-deposits were consumed or not.

Observations of the metallic Mg surfaces used for the Grignard reagent production had been studied by a few groups [9]. Whitesides et al. reported the first observations of metallic Mg surfaces after Grignard reagent formations in 1980 (**Figure 3-2**) [9a]. They observed surfaces of single-crystal magnesium of 99.999+% purity after Grignard reagent formations by Scanned Electron Microscopy (SEM). As the result, spherical or hexagonal pits were formed on the metallic Mg surfaces. These pits grew and eventually overlap. The study revealed that consumption of Mg undertook at peripheries of the formed pits on metallic Mg homogeneously, although inhomogeneously in macro-scale.

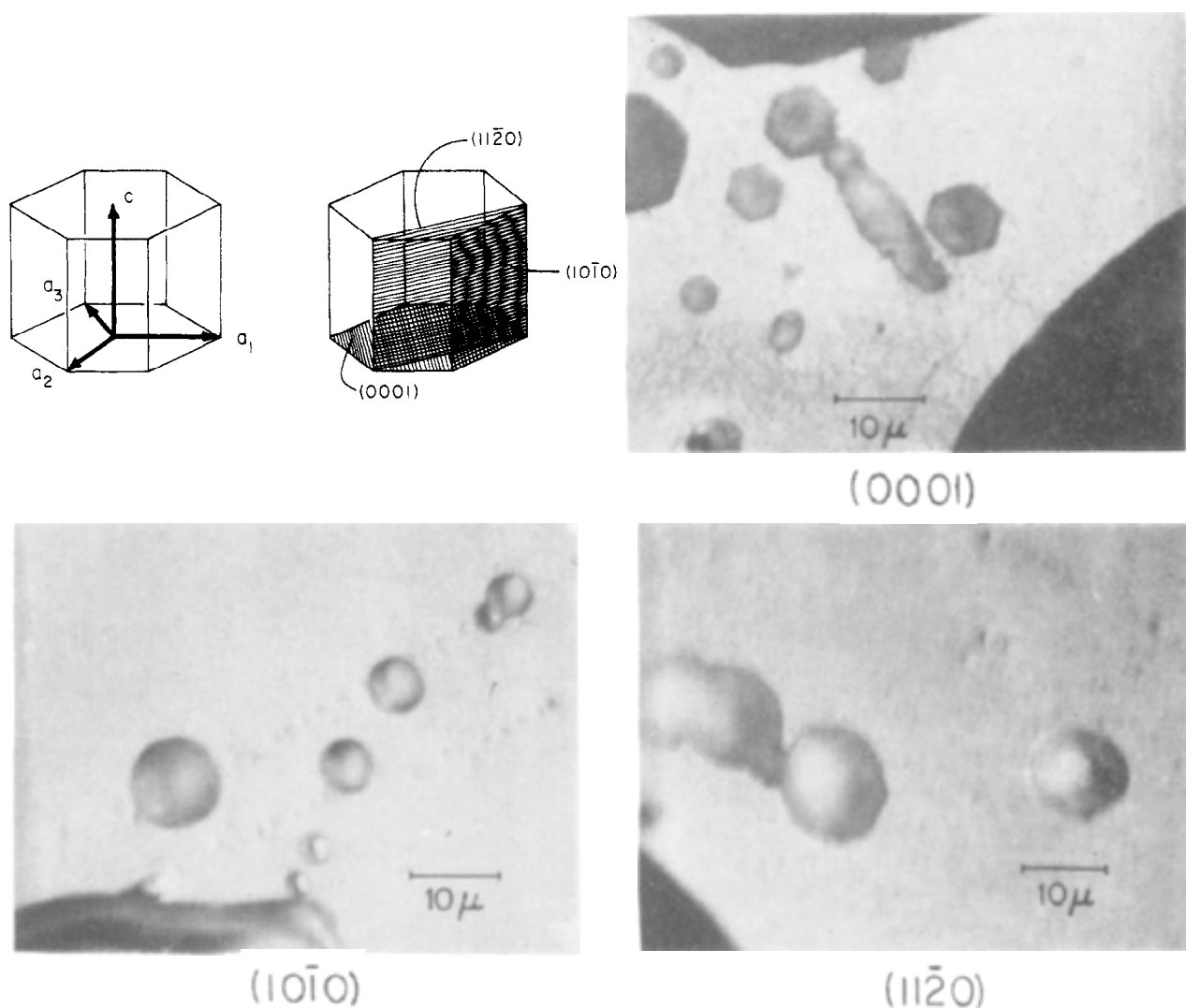


Figure 3-2. The top left figure shows unit cell and the indices of three planes drawn on a unit cell of magnesium. The photographs shows corrosion of the (0001), (10 $\bar{1}$ 0), and (11 $\bar{2}$ 0) planes of magnesium with ethereal 1,4-dibromobutane. The top right photo micrograph shows the hexagonal pits developed on the basal plane, and the lower photomicrographs show the spherical pits developed on the two prismatic planes (10 $\bar{1}$ 0) and (11 $\bar{2}$ 0).

Whitesides et al. have also suggested that the dissolutions of metallic Mg depend on the contacting areas of the Mg(0) atom to solvent molecules (**Figure 3-3**) [9a]. The least energy is required to remove the atom having the smallest number of nearest neighbors. Mg(0) atoms in the metal lattice are less reactive because it requires a large energy to remove neighbor magnesium atoms. Oppositely, one Mg(0) atom surrounded by solvent atoms can be easily dissolved to solvent because it is easily solvated into its Mg²⁺ cation. The more contacting area of the metallic Mg atom to solvent has, the more reactive the metallic Mg atom becomes. Thus, the corrosion of metallic Mg occurs

initially from “kinks and steps” or dislocation of metallic Mg. This would be the reason that the readily dissolved SmI_2 of lower reducing ability can reduce some compounds those cannot be reduced by metallic.

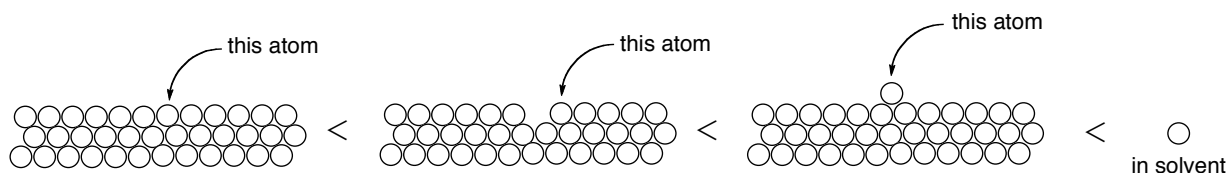


Figure 3-3. The order of reactivity of Mg(0) atom. White circles stand for Mg(0) atoms.

Consumption of Mg(0) atoms in Grignard reagent formations at an atomic level according to the report by Whitesides et al. is illustrated in **Figure 3-4** [9a]. The corrosion of metallic Mg would occur from a disorder on a metal surface as observed. When Mg(0) atoms having larger contact area to solvent react preferentially, pits on metallic Mg grow shallowly and widely. The consumption of Mg toward vertical direction can be explainable by the disorder of the metallic Mg crystal. Every metal or crystal has always disorders in the metal lattice unless it is a perfect crystal.

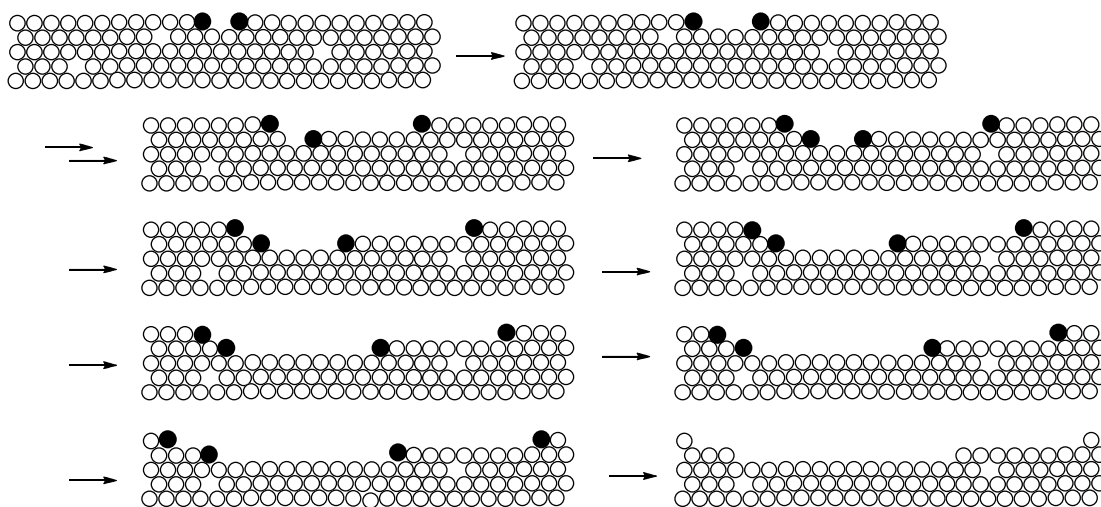
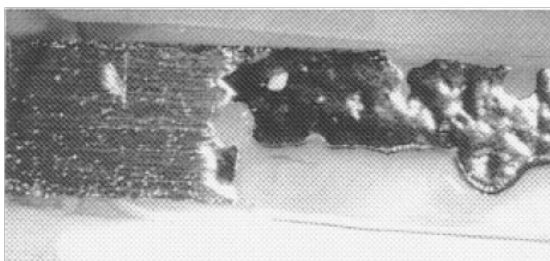


Figure 3-4. A diagram for the corrosion of metallic Mg from the view toward (0001) surface. Black circles are relatively highly reactive Mg atoms. White circles stand for Mg atoms less reactive than Mg atoms represented in black circles. Three or four atoms are consumed in each step.

Observations of the metallic Mg surfaces activated by transition metal (FeCl_3) after the reaction with bromoethane were also reported by Bowyer et al. (**Figure 3-5**) [9c]. The surface of FeCl_3 -treated metallic Mg after Grignard reagent formation from bromoethane was observed in situ by a microscope. The right side of the photograph was the FeCl_3 -treated Mg metal surface after the reaction. The left side of the photograph showed small, discrete reactive sites. In contrast, the FeCl_3 -treated side was almost consumed, and the remaining surface became smooth. In this report, it was concluded that “The Fe(III) is reduced to Fe(0) by the magnesium, and the iron crystal on the surface may act as an initial site of the reaction”. It was mentioned that iron is known to increase side reactions and should be used with caution. Role of the iron in the Grignard reagent formation is obscure.



Teerlinck, C. E.; Bowyer W. J. *J. Org. Chem.* **1996**, *61*, 1059-1064.

Figure 3-5. A magnesium surface after the reaction with bromoethane. Left side was untreated, and the right side was treated with 2% FeCl_3 in THF. The width of field is 11.8 mm.

The surface of the purchased metallic Mg, the metallic Mg surface after being soaked in $\text{Me}_3\text{Si-Cl/THF}$ solution, and metallic Mg surface after the reaction of **1a** in $\text{Me}_3\text{Si-Cl/DMPU}$ solution were shown in **Figure 3-6**, **Figure 3-7**, and **Figure 3-8**, respectively. Metallic Mg before the reaction exhibited a metallic luster. Meanwhile, metallic Mg surface after the reaction of **1a** had black circular pits (approximately 30-40 μm width). One of the pits had several μm -depth. These results showed that consumed region of metallic Mg surface appeared as black region.

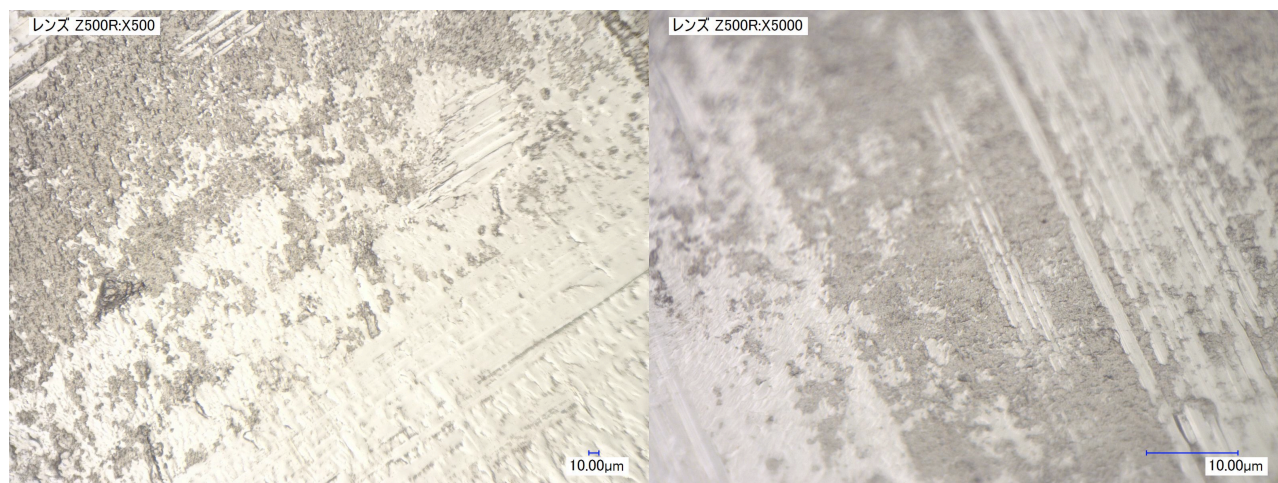


Figure 3-6. Surfaces of purchased Mg ribbon. The photograph of the right side is a magnified picture.



Figure 3-7. Mg surface washed by Me₃Si-Cl in THF. The photograph of the right side is a magnified picture.